# Sea-ice anomalies in the western Arctic and Greenland-Iceland Sea and their relation to an interdecadal climate cycle

Lawrence A. Mysak and Scott B. Power
$C^2$GCR Report No. 92-17
November 1992

CB92 11 Nov 92

# Sea-ice anomalies in the western Arctic and Greenland-Iceland Sea and their relation to an interdecadal climate cycle

Lawrence A. Mysak* and Scott B. Power**

Centre for Climate and Global Change Research
and Department of Atmospheric and Oceanic Sciences
McGill University, Montreal, QC H3A 2K6

Submitted to Climatological Bulletin

November, 1992

---

*Telephone: 514 398 3759; Fax: 514 398 6115

**Present affiliation: Bureau of Meteorology Research Centre, G.P.O. Box 1289K, Melbourne, Vic. 3001, Australia

**Abstract**

From an analysis of Arctic sea-ice concentration, sea-level pressure, runoff and salinity data collected during the 1980s, it is found that large sea-ice extents and low salinities observed in the Greenland-Iceland Sea during the late 1980s can be attributed to prior high runoffs into the Beaufort Sea in the mid-1980s. We refer to such ocean climate freshening events in the Greenland-Iceland Sea as 'Great Ice And Salinity Anomalies' or GIASAs. A lagged cross-correlation study of 36 years of low-pass filtered areal sea-ice extent anomalies from various subregions of the central Arctic Basin and Greenland-Iceland Sea indicates that both positive and negative ice anomalies tend to propagate from the Beaufort Sea through to the Greenland-Iceland Sea via the Beaufort Gyre and the Transpolar Drift Stream. This behaviour of the sea-ice fluctuations is consistent with the interdecadal Arctic climate cycle recently proposed by Mysak, Manak and Marsden. A study of lagged cross-correlations of low-passed filtered ice data from subregions covering the whole Arctic and its marginal seas reveals a complex ice anomaly drift pattern which, however, has a number of similarities with that recently obtained by Chapman and Walsh from an analysis of monthly ice anomalies. A discussion is also given of the possible connections between the decadal-scale GIASAs and lower latitude interdecadal climate variations.

## 1 Introduction

In a recent paper, Mysak et al.(1990, hereafter referred to as M) proposed that decadal-scale fluctuations of sea-ice extent in the Greenland-Iceland Sea may be linked to a certain sequence of high-latitude hydrological, oceanic and atmospheric processes in the form of a multi-component feedback loop (Kellogg 1983). Fig. 1 shows a modified (and simplified) form of this loop, which was also used as the basis of a Boolean Delay Equation model of interdecadal Arctic climate variability (Darby and Mysak 1992). Because the loop is **negative** or **reversing**, it can, in the absence of other strongly damping factors, give rise to self-sustained climatic oscillations in the Arctic with an estimated period (the time to go around the loop twice) of 15-20 years. For example, the loop implies, among other things, that in northern Canada, there can be alternating states of heavy and light runoff, which are followed a few years later by corresponding states of suppressed convection and convective overturning in the Iceland Sea. (We define here the Iceland Sea as the region between Jan Mayen Island (71°N, 8°W - see Fig. 2a) and Iceland. The Greenland Sea, on the other hand, is the region between Jan Mayen and Fram Strait. We shall refer to the two regions collectively as the Greenland-Iceland Sea. In M (and also Mysak and Power 1991) however, the Greeland-Iceland Sea was simply called the Greenland Sea.

The 'Great Salinity Anomaly' or **GSA** (Dickson et al. 1988), a freshening of the North Atlantic subpolar gyre in the late 1960s and 1970s which suppressed convection in the Iceland Sea for

several years, was incorporated into the aforementioned feedback loop by M, who argued that it could have been partly formed by large runoffs into the western Arctic during the mid-1960s (see Fig. 17 in M). Therefore, M proposed that the GSA could be regarded as a cyclic event, part and parcel of a sequence of large-scale air-ice-sea interactions in the Arctic. On the basis of this conceptual model, M also gave evidence of the occurrence of earlier GSA-like events during this century. It was also predicted by M that another GSA-like event would have occurred in the Greenland-Iceland Sea in the late 1980s.

Mysak and Power (1991) showed that consistent with the above prediction, large sea-ice extents did indeed occur in the Greenland-Iceland Sea during February 1987 and 1988. (They also found that over a period of several decades, fluctuations of North American runoff into the Arctic significantly lead the ice anomalies in the Greenland-Iceland Sea by 3-5 yr.) Coincident with the occurrence of the ice anomalies during the late 1980s was the reduction of convection in the Greenland Sea (Rudels et al. 1989; Schlosser et al. 1991) and the appearance of upper-ocean low salinity water there during February and March 1989 (GSP Group 1990). If the latter freshwater anomaly advected southward into the Iceland Sea and suppressed convection there, then taken together, these features suggest that a moderately-sized GSA-type event occurred in the Iceland Sea in the late 1980s. As in the case of the 1960s GSA, the large Greeland-Iceland Sea ice anomalies in the late 1980s appeared to have advected into the Labrador Sea

(see Fig. 7 in Chapman and Walsh 1992) and therefore contributed to the extremely heavy ice conditions and cooler air temperatures along the coast of Newfoundland in May 1991 for example (Globe and Mail, 31 May 1991). (It has also been proposed by J. Elliot (personal communication 1991) that such large ice anomalies could be partly due to anomalous offshore winds which forced the coastal ice seaward.)

The main purpose of this paper is to present evidence which indicates that this last GSA-type event, which we shall call a **GIASA**, an acronym for '**G**reat **I**ce **A**nd **S**alinity **A**nomaly', may have also originated from large runoffs into the western Arctic during the mid-1980s. However, the possible role of anomalous regional surface winds in creating the GIASA is also examined. Dickson et al. (1975) and Walsh and Chapman (1990a) (see also Serreze et al. 1992) have argued, respectively, that anomalous winds over the Greenland Sea and to the northwest of Fram Strait were important forcing factors in the generation of the GSA.

A second purpose of this paper is to present a lagged cross-correlation analysis of 36 years of low-pass filtered sea-ice concentration data from several subregions of the Arctic and marginal seas. The goal here is to show that both positive and negative ice anomalies in the western Arctic propagate out into the Greenland Sea and beyond with the mean ice drift. Also, the low-frequency ice anomaly drift pattern for the whole Arctic and its marginal seas is found and compared with that obtained by Chapman and Walsh (1991) who used monthly data from the US Navy/NOAA Joint

Ice Center subregions.

Finally, the third purpose of this article is to comment on the possible connections betweem GIASAs and lower latitude interdecadal climatic fluctuations. Evidence accrued so far (eg, see the references listed in Weaver et al. 1991) suggests that many types of natural interdecadal fluctuations occur at middle and high latitudes; thus it is conceivable that they could be triggered by polar climatic variations on this time scale. Alternatively, middle latitude fluctuations could influence (eg, amplify) the type of climate oscillations described in M. A better understanding of these connections is particularly relevant to one of the central problems associated with potential greenhouse warming: how to separate natural climate variations on decadal time scales, which tend to be amplified in the north polar region, from those climatic changes due to anthropogenic forcing which occur on the decade-to-century time scale.

The outline of this paper is as follows. In section 2 the data sets that we have analyzed are described, and in section 3 a discussion is given of the 1980s GIASA, which is also compared with the generation and evolution of the GSA in the 1960s. Also in section 3 some new insights are given on what might have caused the large 1960s runoffs into the Arctic, which partly generated the GSA. In section 4 we present a lagged cross-correlation analysis of 36 years of low-frequency areal sea-ice anomalies for various subregions of the Arctic. Finally, in section 5 we suggest how GIASAs may be linked with lower latitude interdecadal climate

variability.

## 2 Data

The sea-ice concentration (SIC) and sea-level pressure (SLP) data that are presented in the next two sections were kindly provided by John Walsh of the University of Illinois. The SIC data consist of end-of-the-month concentrations in tenths given on a square 1°x1° (latitude) grid centred at the north pole, which was developed by Walsh and Johnson (1979). The positive x and y axes of this grid are along 20° W and 70° E, respectively (eg, see Fig. 2 in M). The data cover the period 1953-88, but according to Chapman and Walsh (1991), the quality prior to 1972 is less reliable because then the data were derived from many sources. After 1972 the routine monitoring of sea ice on the hemispheric scale was made possible by polar-orbiting satellites whose passive microwave sensors had cloud penetrating capabilities, and accordingly, the data became much more homogeneous. Maps of the annual mean and seasonal mean SIC fields for each year during the period 1953-88 are given in the 'quick look' atlas of Mysak and Wang (1991).

From the monthly SIC data, areal sea-ice extent anomalies were calculated as described in Mysak and Manak (1989) to remove the 36-year climatological annual cycle. These anomalies were then subdivided to form areal sea-ice anomaly time series for each of the subregions shown in Fig. 2a, which are similar to the US Navy/NOAA Joint Ice Center standard subregions (eg, see Fig. 3 in

Chapman and Walsh 1991). To focus on the low-frequency variability of the areal sea-ice extent anomalies, the time series for the subregions were next low-pass filtered to remove all spectral components with periods shorter than 30 months (see Power and Mysak (1992) for details of the filtering procedure). The resulting smoothed areal sea-ice anomaly time series were used in the cross-correlation analysis in section 4. A set of these time series for the five contiguous subregions $B_1$ to $D_1$ is shown in Fig. 2b. Note that the sequence of subregions follows the ice drift pattern which leads to the export of sea ice out of the Arctic Ocean (through Fram Strait) via the Beaufort Gyre (BG) and the Transpolar Drift Stream (TDS) (see Fig. 18b in M).

The monthly mean SLP data provided by Walsh originate from NCAR and are given on a 5°x5° latitude-longitude grid which covers most of the Northern Hemisphere from January 1899 to January 1988. However, because of missing data in the Arctic prior to the 1950s and the limited record of SIC data, only the data from 1953-87 were used in this paper. Maps of the seasonal mean and annual mean SLP fields for each year are displayed in the 'quick-look' atlas of Mysak and Wang (1991), who also included the SLP anomaly fields (departures from the 1953-87 climatololgy). For a further discussion of the SLP data, we refer the reader to Walsh and Chapman (1990b) who used this data set to study short-term Arctic climate variability. The low-pass filtered SLP data have been analyzed by Power and Mysak (1992).

## 3 The 1980s Great Ice and Salinity Anomaly (GIASA)

The large Greenland-Iceland Sea ice extents shown in Mysak and Power (1991) for February 1987 and 1988 are also clearly visible in the winter (the mean of December, January and February) SIC maps for 1987 and 1988 (see pp. 152 and 155 in Mysak and Wang (1991)). A characteristic magnitude of the associated low-pass filtered areal sea-ice anomalies in the late 1980s is $6 \times 10^4$ km$^2$ (see the $D_1$ time series in Fig. 2b), which when multiplied by the typical ice thickness for this region (1 m - see Bourke and Garrett 1987), gives a characteristic ice volume anomaly magnitude of 60 km$^3$. If this 1980s GIASA is an integral part of the interdecadal cycle illustrated in Fig. 1, then conceivably, like in the case of the GSA, it too could have been partly generated by large runoffs into the western Arctic during the mid-1980s.

Figure 3a shows that during 1984-86 the Mackenzie River discharge was indeed above average, a situation which presumably caused the simultaneous below-average salinities on the Beaufort shelf to the north of the Mackenzie delta (Fig. 3b) and also the positive areal sea-ice anomalies in the western Arctic subregion $B_1$ (Fig. 3c). The runoff-ice cover relationship is consistent with the findings of Manak and Mysak (1989) who showed, among other things, the the Mackenzie River discharge is positively correlated with ice extent on the Beaufort Sea shelf, with discharge leading by about one year. (The basic mechanism believed operative here is that fresher upper-ocean water due to higher runoff tends to freeze more easily and hence produce more sea ice the following winter and

spring.) The ice anomaly in the Beaufort Sea has a magnitude of about $3x10^4$ $km^2$ (Fig. 3c), and since the ice thickness is typically 2-3 m here (Bourke and Garrett 1987), the corresponding ice volume anomaly is 60-90 $km^3$, which is comparable to that in the Greenland-Iceland Sea, as estimated in the previous paragraph.

From Fig. 3c it is also interesting to note the large ice anomaly peak in 1975, which is most likely due to the very high runoff (Fig. 3a) and low shelf salinities (Fig. 3b) in 1974. On the other hand, the largely negative ice anomalies during 1978-82 appear to have been caused by the low runoffs and high salinities which occurred at about that time. Finally, in the earlier part of the ice anomaly time series in Fig. 3c, we observe the large positive anomalies during 1964-67, which M proposed were caused by the anomalously large runoffs from North America into the Arctic (Fig. 17 in M).

It is instructive at this point to compare particular annual mean SIC maps with corresponding SLP maps in order to determine, in a crude way, the possible role of atmospheric forcing in creating the ice anomalies, first in the western Arctic and then in the Greenland Sea a few years later. Upon comparing Figs. 4a and 4b, we first note that in the Beaufort Sea region the ice coverage during 1985 was above average, which is consistent with Fig. 3c. Upon comparing Figs. 4d and 4e we observe that during 1985 there was a high pressure anomaly cell over the western Arctic, whose associated (anomaly) winds would, in the absence of other factors, have tended to produce ice convergence, resulting in lower ice

concentrations in the coastal region of the Beaufort Sea since the ice motion would tend to be a few degrees to the right of the local wind vectors. However, in reality the SIC was above average along the coast, which signifies that runoff-induced ice formation (Manak and Mysak 1989) dominated the aforementioned wind-driven effect.

From a comparison of Fig. 4c and 4a we see that during 1987, two years after the positive anomalies in the western Arctic could have been advected into the Greenland-Iceland Sea via the BG and TDS (see line $L_4$ Fig. 2b and section 4), the ice edge in the Greenland Sea (ie, north of Jan Mayen) is much further south than in climatology. We also note that the SIC is considerably reduced in the Beaufort Sea. During 1987 there was also a high pressure anomaly cell over the Greenland-Iceland Sea (Fig. 4f), whose associated winds would have tended to drive the ice edge <u>toward</u> the east Greenland coast. Remarkably, however, this process did not create a negative ice-extent anomaly in the Greenland-Iceland Sea. Thus we conclude that the ice enhancement processes in the Arctic basin (especially that due to runoff) were sufficiently strong to produce enough ice there which when exported into the Greenland-Iceland Sea, dominated the wind-driven effects.

In the case of the 1960s GSA, runoff and wind driven effects appeared to have worked together in creating the large ice anomalies, first in the western Arctic and then in the Greenland-Iceland Sea. Fig. 5a shows a nearly solid ice cover in the western Arctic during 1964 (a very large runoff year), which could, however, also have been partly created by the weak low pressure

anomaly cell over this region (see Fig. 5c, right) because the associated anomaly winds in this case would have produced ice divergence, ie driven the thick, multi-year ice in the central Beaufort Sea toward the coast. Similarly, during 1968 the extensive sea-ice cover in the Greenland-Iceland Sea could have been partly created by the anomaly winds associated with the high pressure anomaly cell whose centre is to the west of Iceland (Fig. 5d, right), as originally proposed by Dickson et al. (1975). We also note here that the winds associated with the mean annual SLP field for 1967 (Mysak and Wang 1991) would have driven the thick multi-year ice north of Greenland into the TDS which could have added to the large sea-ice extent seen in Fig. 5b (as first suggested by Walsh and Chapman (1990a)). The fact that the 1968 ice volume anomaly in the Greenland-Iceland Sea is at least 200 $km^3$ (versus about 100 $km^3$ for the Beaufort Sea ice anomaly - see Fig. 2b) further confirms that the regional winds were an important contributor to the large sea-ice anomalies seen in subregion $D_1$ at that time.

Clearly, further research is required to sort out the relative importance of the different mechanisms that generate GIASAs. Also, the fact that the atmospheric circulation over the Greenland-Iceland Sea during the peak of the GSA was different than that during the 1980s GIASA indicates the possible importance of lower latitude influences. Work on this problem is currently in progress at McGill (D. Holland, pers. comm., 1992) where an atmospherically driven coupled ice-ocean model of the Arctic and North Atlantic is

being run to test the efficacy of the different ice generation and forcing mechanisms described above.

Critics of the interdecadal Arctic cycle theory proposed by M and now embodied in Fig. 1 often argue that anomalies in the runoff from the Siberian rivers, whose total climatological discharge is four to five times that of the Mackenzie (Aagaard and Carmack 1989), should contribute substantially to the formation of GIASAs. It is countered here that because of the very wide and shallow Eurasian shelf, any anomalies from this runoff get well mixed on the shelf with central Arctic Ocean waters that flow up onto the shelf. After mixing due to eddies and convective overturning, the waters near the edge of the shelf then tend to slide down into the intermediate Atlantic layer of the Arctic (Coachman and Barnes 1962) and hence do not directly affect ice formation at the surface. Also, as pointed out in M, during the years of peak runoff from North America in the mid-1960s, the Siberian runoff was near normal or below normal (Cattle 1985), and hence could not have added to the fresh water anomalies that made up the GSA.

Other possible weaknesses of the feedback loop in Fig. 1 are the following two links: First, that strong convective overturning during winter in the Iceland Sea (a process which would create positive SST anomalies because of the warm Atlantic water being brought to the surface, and hence cause increased heat fluxes to the atmosphere in this region and, because of ocean advection of the SST anomalies, also cause increased heat fluxes in the Irminger Basin) would produce strong cyclogensis around Iceland (see left

side of Fig. 1). Secondly, that such cyclogensis would contribute to increased precipitation and runoff in northern Canada (see upper left and top part of Fig. 1). At this stage we cannot easily verify the first link; however, an examination of winter SLP maps for the years just before the GSA suggests how greater precipitation (and hence runoff) in northern Canada could have resulted from a change in the position and structure of the Icelandic Low. We also suggest that the occurrence of this latter link is consistent with the recent 'teleconnection' results of Walsh and Chapman (1990b). The showed that the winter SLP anomalies in the Iceland Sea and Irminger Basin are highly correlated ($0.6 < r < 0.8$) with those at the 'base point' 75°N, 90°W in the CAA (see their Fig. 12b).

From the orientation of the isobars on the northern side of the climatological Icelandic Low (Fig. 6a), we observe that cold dry air would tend to flow southward from the eastern Arctic into the Greenland Sea, then westward across Greenland and finally southward over the Canadian Arctic Archipelago (CAA) and Hudson Bay. (Although the Greenland ice sheet is about 2 km above sea level, since the troposphere is over 10 km thick in this region one would expect at least some of the low-level flow around the Iceland Low to pass over the ice sheet.) Similarily, on the western side of the CAA there would tend to be a northerly flow of cold dry air from the Arctic High region in the western Arctic. Taken together we would thus expect fairly low precipitation and runoff in northern Canada. During winter 1961 the Icelandic Low and the

Arctic High both intensified, but there was little change in their positions or in the orientation of their isobars (see Fig. 6b). Thus we would have expected even more cold dry air over northern Canada and consequently, very low precipiation and runoff into the Arctic Ocean and Hudson Bay. The latter was indeed observed during - see Fig. 17 in M.

Figure 6c on the other hand, shows that quite a different situation occurred with respect to the SLP pattern during winter 1964 (the year of maximum runoff), presumably because of changes in the ocean-to-atmosphere heat fluxes around Iceland. The Icelandic Low broke up into two lows (see Fig. 6c, left), with the centre of the main (southern) low being located south of Greenland. Also the orientation of the isobars south of Iceland implies that warm moist air from west of the United Kingdom (where the SSTs are typically 10° C) would have been transported across and around southern Greenland and over to the CAA and Hudson Bay, and hence have caused heavy precipitation and large runoffs there, as observed (Fig. 17 in M). The existence of such easterly anomaly winds around the southern end of Greenland when the main centre of the Icelandic Low shifts southward has also been noted by Dunbar and Thomson (1979). At the same time, it is interesting to note that the Aleutian Low intensified and its centre shifted westward during winter 1964, which would have also brought in warm moist air from the Pacific to the western part of northern Canada (see Fig. 6c, right) and hence contributed to the large runoff. Remarkably, a similar situation regarding the SLP pattern also occurred during winter 1965 (Mysak

and Wang 1991), which was another year of high runoff (see Fig. 17 in M).

It is now instructive to compare the above SLP patterns with those that occurred during the winters of 1968-70, the peak GSA years when convective overturning was suppressed in the Iceland Sea and the SST anomalies were negative (see Fig. 6 in M). During these winters, there were strong northerly flows of cold dry air along the east coast of Greenland (Dickson et al. 1988; Mysak and Wang 1991) and a high pressure anomaly cell over the CAA (this can also be seen in Fig. 5d, which shows the annual SLP field and its anomalies for 1968). As a consequence, a higher incidence of anticyclones over the CAA would have been expected, and indeed this occurred (Serreze et al. 1992). Also, this would imply lower runoffs in northern Canada at that time; this was certainly the case for the Mackenzie River in 1969 and 1970 (see Fig. 21 in Tyler (1992)).

Just before the time of the most recent GIASA, a sequence of SLP patterns similar to those in the mid-1960s also occurred. The patterns of the winter 1985 and 1986 SLP maps (Mysak and Wang 1991) imply that warm moist air from the southeast of Greenland would have been transported across southern Greenland and into northern Canada, causing heavy precipitation and large runoffs, as observed (Fig. 3a). As more data becomes available it will be interesting to examine the evolution of the SLP fields and runoffs during the late 1980s (peak GIASA years), to see if that was also a period of more anticyclones and lower runoffs in northern Canada.

## 4 Lagged Cross-correlation Analysis of Subregion Anomalies

From the sloping lines $L_i$ in Fig. 2b, we note several cases in which both positive and negat from the Beaufort Sea through to the Greenland Sea, with a travel time of the order of 2-3 years. This suggests it worthwhile to perform a lagged cross-correlation analysis of the ice anomalies in the subregions linking these two seas. The procedure we follow is similar to that used by M, who studied the movement of smoothed Greenland-Iceland Sea ice anomalies into the Labrador Sea via five subregions (see their Figs. 2 and 3). Later in this section we shall also present the results of cross-correlation calculations for other subregions which yield a picture of the ice anomaly advection pattern for the whole Arctic Ocean and its marginal seas. However, it should be pointed out that not all anomalies are created in the western Arctic and then propagated out into the Greenland-Iceland Sea. For example, the large negative ice anomalies centered around 1984 in subregions $B_4$ and $D_1$ were likely caused by the anomalous winds assoiciated with 1984 SLP pattern over the eastern Arctic (see Fig. 14 in Chapman and Walsh 1991) which would have tended to push ice in the TDS over towards the north of Greenland.

In the first phase of the analysis, the lagged cross-correlation functions were computed for the low-pass areal ice anomalies in subregion $B_1$ versus those in the subregions $B_2$, $B_3$, ... $D_3$, a sequence which follows the mean ice drift from the Beaufort Sea through to the Labrador Sea. These functions were next examined for asymmetries about the zero-lag to determine direction

of anomaly advection (Chapman and Walsh 1991; see also Fig. 4 in M). The maximum lagged correlation coefficients obtained from this analysis are given in Table 1. To find the 95% significance level for the correlations, the number of degrees of freedom (for simultaneously correlated data) was first estimated to be 2N/30 = 29, where N = 432 (total number of months of data) and 30 is the high-frequency cutoff. Then from Table 13 in Pearson and Hartley (1966), we obtained, using a one-tailed test for normally distributed data, a 95% significance level of approximately r = 0.3. This simple method for determining the significance level was deemed to be satisfactory when compared with results using the more sophisticated approach adopted by Power and Mysak (1992). For lagged cross-correlations, the number of degrees of freedom decreases with lag and the significance level for r slowly increases to 0.36 for a lag of 120 months. This is due to the fact that as the lag increases, less data are used in the calculation of the cross correlations.

The results of Table 1 show that the low-frequency ice anomalies in $B_1$ lead those in the Greenland Sea (subregion $D_1$) by just over two years, which is consistent with the phase lines shown in Fig. 2b. Moreover, there appears to be a continuous advection of ice anomalies by the BG, the TDS and the EGC (East Greenland Current) all the way into the Labrador Sea. (Although the maximum cross-correlations for data from $B_1$ versus $D_2$ and $D_3$ are not significant, the cross-correlations between the data from adjacent regions are significant (see Fig. 8b below) and thus support the

above conclusion.)

To estimate the average speed of advection of the ice anomalies from the Beaufort Sea into the Greenland Sea and beyond, a cumulative lag plot was constructed (Fig. 7). From the best linear fit to the data, we find an average advection speed of about 2000 km/yr, or roughly 5 km/day, which lies well within the range of typical drift speeds for sea ice, namely 1 - 10 km/day (Chapman and Walsh 1991).

Chapman and Walsh (1991) determined the monthly ice anomaly drift pattern for the whole Arctic (Fig. 8a) by computing the lagged cross-correlation functions for data from adjacent US Navy/NOAA Arctic subregions (indicated by the heavy lines in Fig 8a). These differ from those defined in Fig. 2a as follows: The Navy/NOAA Arctic Ocean subregion approximately consists of the union of $B_1$ to $B_5$; their Southern Baffin Bay subregion consists of $D_3$ and $D_4$; and their Bering Sea consists of $S_1$ and $S_2$. On the other hand, the CAA subregion in Fig. 2a has been subdivided into West Canada and East Canada in the Navy/NOAA scheme. However, even with these differences it is possible to make a comparison of the Chapman and Walsh ice anomaly drift pattern with that obtained here (Fig. 8b), which is based on the cross-correlations between the low-pass filtered time series from the subregions in Fig 2a.

First, we note from Fig. 8a that the monthly ice anomalies in the Beaufort Sea also appear to propagate all the way to the Irminger Basin (subregion $D_2$), as was found for the low-pass anomalies (Figs. 7 and 8b). However, the lack of resolution for

the Labrador Sea region in the Navy/NOAA scheme probably accounts for the absence of anomaly propagation from the Irminger Basin into the this region. In both patterns we observe an eastward drift of the anomalies along the Eurasian shelf; however, we note that the subregion $S_3$ (Chukchi Sea) appears to be a source region for the low-frquency anomalies (see Fig. 8b). Other notable differences are the propagation of low-pass filtered anomalies from the Chukchi Sea into the Bering Sea; from the Beaufort Sea into the CAA; and from the subregions $B_5$ and BB into the CAA. No significant such correlations were found by Chapman and Walsh, which suggests that at relatively low frequencies there may be important 'teleconnections' between these subregions. The Chukchi-Bering Sea connection is reminiscent of the results of Power and Mysak (1992) who found that the teleconnection between the western Arctic SLP anomalies and those in the Pacific became more pronounced at longer periods (greater than five years).

Another interesting relationship found in the cross-correlation analysis of the low-pass filtered anomalies is that the fluctuations in Hudson Bay significantly lead those in the Labrador Sea. (Since these two regions are separated by Hudson Strait, no connecting arrow is shown in Fig. 8b.) Chapman and Walsh, however, found that the monthly ice anomalies in the Labrador Sea slightly lead those in the Hudson Strait-Hudson Bay region (see Fig. 8a).

## 5 Possible Connections of GIASAs with Lower Latitude Interdecadal Variability

In reality it is quite likely that the interdecadal Arctic climate cycle depicted in Fig. 1 may be connected to lower latitude decadal-scale fluctuations in the atmosphere and oceans. This idea is in part supported by the findings of Power and Mysak (1992) who showed that statistically significant associations exist between Arctic and extratropical SLP fluctuations, especially at periods of several years. In the way of connections there are (at least) three possibilities: 1) The Arctic cycle triggers lower latitude fluctuations. 2) Lower latitude variations influence or excite some of the processes involved in the feedback loop shown in Fig. 1. 3) There are lower latitude decadal-scale fluctuations that co-exist with the interdecadal Arctic climate cycle. We now expand on each of these cases.

### 5.1 The Arctic as a trigger for lower latitude fluctuations

Because the Greenland Sea is weakly stratified, the waters there are "delicately poised with respect to their ability to sustain convection" (Aagaard and Carmack 1989). Hence these authors have argued that a modest increase in the supply of fresh water from the Arctic could reduce convection in the Greenland Sea. However, it is not believed (R. Dickson, pers. comm. 1992) that this occurred during the time of the GSA. It was only in the Iceland Sea to the south that convection was suppressed during the early years of the GSA.

However, it is conceivable that alternating periods of

extensive and reduced ice cover in the Greenland-Iceland Sea, which are respectively accompanied by relatively cold and warm upper-ocean temperatures (see Fig. 6 in M), could result (via advection) in decadal-scale sea surface temperature (SST) anomalies in the southwestern part of the subpolar gyre (Mysak 1991). It is important to determine the origin of such SST anomalies since they generate significant large-scale disturbances in the overlying atmosphere (Palmer and Sun 1985) and also appear to influence runoff in western Siberia (Peng and Mysak 1992).

From Fig. 9, which depicts the time-longitude evolution of SST anomalies averaged over a mid-latitude band in the North Atlantic, we clearly see the existence of alternating cold and warm periods in the northwestern Atlantic, ie, at around 30°W. Along the time axis, the sequence of solid and dotted lines indicate respectively, large and small (or near-normal) sea-ice extents in the Greenland and Iceland Seas. In several cases, we observe that heavy ice conditions (large sea-ice extents) preceed negative SST anomalies in the northwestern Atlantic by approximately 5 years (the advection time from the Greenland-Iceland Sea to this region via the subpolar gyre), and similarly, light ice conditions in the Greenland-Iceland Sea preceed positive SST anomalies, also by about 5 years. While the correspondence between heavy (light) ice conditions and relatively cold (warm) SSTs in the northwestern Atlantic is not completely one-to-one, the relationship is sufficiently encouraging to warrant further investigation. It is also relevant to point out here that the most prominent

interdecadal periodicity associated with the ice anomalies in the Greenland-Iceland Sea, as determined from the spectrum of the 375-year Koch ice index for Iceland, is 27 years (Stocker and Mysak 1992).

Another way in which Arctic sea-ice changes could cause lower latitude climate variability is via the surface albedo: anomalously large sea-ice extents increase the albedo and vice-versa. However, the changes in ice area on decadal time scales (as opposed to those due to the seasonal cycle) are only of the order of a few percent (Mysak and Manak 1989), and therefore are unlikely to induce very large changes in the Arctic energy budget, which impacts upon the energy budget of the middle latitudes via the circulation in the troposphere. On the other hand, the southern hemisphere sea-ice cover, because it is thinner and closer to the equator, may show larger changes on the decadal time scale. Thus the discussion of decadal-scale Arctic albedo changes should be done in concert with studies of the natural variability of the south polar region.

## 5.2 Forcing from the lower latitudes

The second possibility, that lower latitude interdecadal fluctuations excite similar-scale Arctic climate changes is the more traditional and widely accepted viewpoint. There have recently been many observations of interdecadal variability at middle and tropical latitudes in the climate system (for a list of references, see Weaver et al. 1991). Many investigators believe that these fluctuations may be due to internal oscillations in the

thermohaline circulation (THC), an idea that goes back to Bjerknes (1964). Remarkably, climate modellers have shown that these THC oscillations can occur even in the presence of steady atmospheric forcing (eg, see Weaver et al. (1991) and the references therein). Such oscillations would produce fluctuations in the oceanic poleward heat transport and hence cause changes in surface air temperature at locations where the THC 'ventilates' - in the northern North Atlantic and in the Southern Ocean. Such poleward heat transport changes in the North Atlantic, which could also have contributed to the SST anomalies seen in Fig. 9, have recently been observed by Greatbatch and Xu (1992). They found increased transports at 54.5°N in the 1950s and reduced tranports in the 1970s, which correspond to the warm and cold SSTs seen at these times in Fig. 9.

In the recent study of Higuchi et al. (1991), it was shown that the standing eddy poleward heat transport in the lower troposphere in the northern hemisphere exhibits strong decadal-scale variability. In particular, in years of very large (weak) transports, they found that the ice margin in the Greenland Sea is substantially reduced (expanded). Thus the atmosphere in this case is the medium which can transmit lower latitude decadal-scale signals into the Arctic region and possibly alter the circulation there. This concept is certainly consistent with the aforementioned fact (section 3) that the SLP anomalies over the Greenland Sea in 1968 (peak GSA year) and in 1987 (peak GIASA year) were quite different and hence could have been due to lower

latitude variabilities, independent of air-sea interactions around Iceland (see also Dickson and Namias 1976).

5.3 Co-existing Arctic and lower latitude fluctuations

The third possibility, that polar and lower latitude decadal-scale climate fluctuations may simply 'co-exist', is suggested by the spatial structure of the third empirical orthogonal function (EOF) of SST anomalies that has been computed by Folland et al. (1986a) (see bottom of Fig. 10, which also shows for comparison the first 'global warming' EOF and the second 'ENSO' EOF - see Bryan and Stouffer (1991)). Note that the largest amplitudes of the third EOF, whose temporal fluctuations have an interdecadal time scale, are in the northeast Pacific, the northwest Atlantic and in a broad band over the South Atlantic and South Indian oceans. This high-latitude amplification suggests as well, perhaps, that the global THC (the 'conveyor belt') may be a connecting link since the latter is driven by DWF in both the North Atlantic and the Southern Ocean. (As an aside, Folland et al. (1986b) found that such decadal-scale SST fluctuations were closely linked with rainfall changes in the Sahel.)

The particularly large gradients in the northeast Pacific and northwest Atlantic seen in the third EOF of Fig. 10 also indicate that these areas could be closely tied in with interdecadal variability in the Arctic. Walsh and Chapman (1990b) showed that monthly Arctic SLP fluctuations in winter are associated or 'teleconnected' with SLP changes in the northern North Atlantic. In a continuation of this study using data from all seasons, Power

and Mysak (1992) found that at low frequencies (periods longer than five years), this teleconnection pattern persists. But they also discovered a new teleconnection pattern between centres in the Arctic and the North Pacific. However, neither of these statistical studies can address the question of cause and effect, and therefore, these patterns have to be taken as starting points for further research on the global connections of interdecadal climate variability in various regions.

## 6 Summary and Concluding Remarks

We have shown that during the late 1980s, a Great Ice And Salinity Anomaly (GIASA) in the Greenland-Iceland Sea was most likely generated remotely by prior above-average runoffs into the western Arctic Ocean. Similarly, large runoffs also occurred from North America into the Arctic a few years prior to the late 1960s peak of the GSA. However, unlike in the case of the GSA, when regional atmospheric forcing also contributed to its generation, the wind anomalies associated with the SLP fields during the 1980s GIASA would have tended to oppose the formation of large sea-ice extents in the Greenland-Iceland Sea.

A lagged cross-correlation analysis of 36 years of low-pass filtered SIC data from various subregions in the Arctic and marginal seas revealed that ice anomalies are advected in a manner similar to that found by Chapman and Walsh (1991) who used monthly (unsmoothed) data. However, some differences were found; for example, we showed that the Chukchi Sea appears to be a source

region (a 'factory') for low-frequency ice anomalies.

While many of the above results are encouraging in so far as they lend further support for the existence of the interdecadal Arctic climate cycle proposed by M and now described in Fig. 1, more work is required. For example, we have undoubtedly invoked an oversimplified view of runoff-shelf water-ice interactions in the Beaufort Sea. Macdonald and Carmack (1991) have recently examined these interactions in some detail, and certain aspects of their results could be incorporated into the feedback loop shown in Fig. 1. Secondly, with only 36 yr of SIC data available at the time this research work was done, there are some concerns regarding the statistical significance of the cross-correlation results using low-pass filtered data. In a few years, more that 40 yr of SIC and SLP data will be available and thus it would be of considerable interest to redo the analysis described in section 4. Recently, Chapman and Walsh (1992) have analyzed 38 years of SIC data (up to 1990) and showed, among other things, that the recent GIASA definitely had its peak in 1987-88 (see their Fig. 7a).

Finally, we have made a number of speculative comments regarding the possible connections between a) cyclogensis around Iceland and runoff in northern Canada (section 3), and b) GIASAs and lower latitude interdecadal climate variability (section 5). While these remarks should be treated as tentative, it is nevertheless hoped that they will serve as a guide for further studies of regional and global interdecadal variability in the climate system. It is clear however, that to derive statistically

significant results from such studies, we shall need long records of various climate or proxy climate variables, and hence it is important that we develop and support long-term observational climate projects in the Arctic.

**Acknowledgements**

We thank John Walsh and Bill Chapman for providing the sea-ice and atmospheric data and for helpful discussions, Ann Cossette for typing parts of the manuscript, Ursula Seidenfuss for drafting some of the figures and David Holland for reading and commenting on a draft of this paper. LAM is grateful for the research grant support received from the Canadian Natural Sciences and Engineering Research Council and Atmospheric Environment Service, the Quebec Fonds FCAR and the US Office of Naval Research (Code 1122ML).

## REFERENCES


Aagaard, K. and E.C. Carmack, 1989. On the role of sea ice and other fresh water in the Arctic circulation. Journal of Geophysical Research, **94**:14485-14498.

Bjerknes, J., 1964. Atlantic Air-Sea Interaction. Advances in Geophysics, **10**:1-82.

Bourke, R.H. and R.P. Garrett, 1987. Sea ice thickness distribution in the Arctic Ocean. Cold Regions Science and Technology, **13**:259-280.

Bryan, K. and R. Stouffer, 1991. A note on Bjerknes' hypothesis for the North Atlantic variability. Journal of Marine Systems, **1**:229-241.

Cattle, H., 1985. Diverting Soviet rivers: Some possible repercussions for the Arctic Ocean. Polar Record, **22**:485-498.

Chapman, W.L. and J.E. Walsh, 1991. Long-range prediction of regional sea ice anomalies in the Arctic. Weather and Forecasting, **6**:271-288.

Chapman, W.L. and J.E. Walsh, 1992. Recent variations of sea ice and air temperature in high latitudes. Bulletin of the American Meteorological Society, **73**: in press.

Coachman, L.K. and C.A. Barnes, 1962. Surface water in the Eurasian Basin of the Arctic Ocean. Arctic, **15**:251-274.

Darby, M.S. and L.A. Mysak, 1992. A Boolean Delay Equation model of an interdecadal Arctic climate cycle. Climate Dynamics, in press.

Dickson, R.R. and J. Namias, 1976. North American influences on the circulation and climate of the North Atlantic sector. Monthly Weather Review, **104**:1255-1265.

Dickson, R.R., H.H. Lamb, S.A. Malmberg and J.M. Colebrook, 1975. Climatic reversal in the northern North Atlantic. Nature, **256**:479-482.

Dickson, R.R., J. Meinke, S.A. Malmberg and A.J. Lee, 1988. The "Great Salinity Anomaly" in the northern North Atlantic 1968-1982. Progress in Oceanography, **20**:103-151.

Dunbar, M.J. and D.H. Thomson, 1979. West Greenland salmon and climatic change. Meddelelser om Grønland Bd. **202**, Nr. 4, 19pp, København.

Fissel, D.B. and H. Melling, 1990. Interannual variability of oceanographic conditions in the southeastern Beaufort Sea. Canadian Contracter Report of Hydrography and Ocean Sciences No. 35, 102 pp (+ 6 microfiche).

Folland, C.K., D.E. Parker, M.N. Ward and A.W. Coleman, 1986a. Sahel rainfall, northern hemisphere circulation anomalies and the worldwide sea temperature changes. Memorandum 7A, Long Range Forecasting Climate Research, Meteorological Office, Bracknell, U.K., 49 pp.

Folland, C.K., T.N. Palmer and B.E. Parker, 1986b. Sahel rainfall and worldwide sea temperatures, 1901-85. Nature, 320:602-607.

Greatbatch, R.J. and J. Xu, 1992. Interpentadal changes in the transport of volume and heat through sections across the North

Atlantic. Journal of Geophysical Research, submitted.

GSP Group, 1990. Greenland Sea Project: A venture toward improved understanding of the ocean's role in climate. Eos Transactions, American Geophysical Union, 71: No. 4, June 12, 750-754.

Higuchi, K., C.A. Lin, A. Shabbar and J.L. Knox, 1991. Interannual variability of the January tropospheric meridional eddy sensible heat transport in the northern latitudes. Journal of the Meteorological Society of Japan, 69:459-472.

Kellogg, W.W., 1983. Feedback mechanisms in the climate system affecting future levels of carbon dioxide. Journal of Geophysical Research, 88:1263-1269.

Macdonald, R.W. and E.C. Carmack, 1991. The role of large-scale under-ice topography in separating estuary and ocean on an Arctic shelf. Atmosphere-Ocean, 29:37-53.

Manak, D.K. and L.A. Mysak, 1989. On the relationship between Arctic sea-ice anomalies and fluctuations in northern Canadian air temperature and river discharge. Atmosphere-Ocean, 27:682-691.

Mysak, L.A., 1991. Current and future trends in Arctic climate research: Can changes in the Arctic sea ice be used as an early indicator of global warming? Centre for Climate and Global Change Research Report No. 91-1, McGill University, Montreal.

Mysak, L.A. and D.K. Manak, 1989. Arctic sea-ice extent and anomalies, 1953-84. Atmosphere-Ocean, 27:376-405.

Mysak, L.A. and S.B. Power, 1991. Greenland Sea ice and salinity anomalies and interdecadal climate variability. Climatological Bulletin, 25:81-91.

Mysak, L.A. and J. Wang, 1991. Climatic Atlas of seasonal and annual Arctic sea-level pressures, SLP anomalies and sea-ice concentrations, 1953-88. Centre for Climate and Global Change Research Report No. 91-14, McGill University, Montreal.

Mysak, L.A., D.K. Manak and R.F. Marsden, 1990. Sea-ice anomalies observed in the Greenland and Labrador Seas during 1901-1984 and their relation to an interdecadal Arctic climate cycle. Climate Dynamics, 5:111-133.

Palmer, P.N. and Z. Sun, 1985. A modelling and observational study of the relationship between sea surface temperature in the north-west Atlantic and the atmospheric general circulation. Quarterly Journal of the Royal Meteorological Society, 111:947-975.

Pearson, E.S. and H.O. Hartley, 1966. Biometric Tables for Statisticians, Volume 1. Cambridge, 270 pp.

Peng, S. and L.A. Mysak, 1992. A teleconnection study of interannual sea surface temperature fluctuations in northern North Atlantic and precipitation and runoff over western Siberia. Journal of Climate, in press.

Power, S.B. and L.A. Mysak, 1992. On the interannual variability of Arctic sea-level pressure and sea ice. Atmosphere-Ocean, in press.

Rudels, B., D. Quadfasel, H. Frierich and M.-N. Hossaias, 1989.

Greenland Sea convection in the winter of 1987/88. Journal of Geophysical Research, 94:3223-3227.

Schlosser, P., G. Bönisch, M. Rhein and R. Bayer, 1991. Reduction of deep water formation in the Greenland Sea during the 1980s: Evidence from tracer data. Science, 251:1054-1056.

Serreze, M.C., J.A. Maslanik, R.G. Barry, and T.L. Demaria, 1992. Winter atmospheric circulation in the Arctic Basin and possible relationships to the Great Salinity Anomaly in the northern North Atlantic. Geophysical Research Letters, 19:293-296.

Stocker, T.F. and L.A. Mysak, 1992. Climatic fluctuations on the century time scale: A review of high-resolution proxy data and possible mechanisms. Climatic Change, 20:227-250.

Tyler, R., 1992. The potential for using geomagnetic data as proxy for river discharge into the Arctic and a review of other potential proxies. Centre for Climate and Global Change Research Report No. 92-16, McGill University, Montreal.

Walsh, J.E. and W.L. Chapman, 1990a. Arctic contribution to upper-ocean variability in the North Atlantic. Journal of Climate, 3:1462-1473.

Walsh, J.E. and W.L. Chapman, 1990b. Short-term climate variability of the Arctic. Journal of climate, 3:237-250.

Walsh, J.E. and C.M. Johnson, 1979. An analysis of Arctic sea ice fluctuations. Journal of Physical Oceanography, 9:580-591.

Weaver, A.J., E.S. Sarachik and J. Marotzke, 1991. Freshwater flux

forcing of decadal and interdecadal oceanic variability. Nature, 353:836-838.

**TABLE 1:** Maximum lagged cross-correlation coefficients (r) for smoothed areal sea-ice anomalies in subregion $B_1$ (see Fig. 2a) versus those in subregions $B_2$, $B_3$, $B_4$, $D_1$, $D_2$ and $D_3$ (first line). The lag at each maximum correlation is given in the second line. The 95% significance level is estimated to be approximately r = 0.3 for simultaneously correlated data, rising to 0.36 for data sets lagged up to 120 months.

| | $B_2$ | $B_3$ | $B_4$ | $D_1$ | $D_2$ | $D_3$ |
|---|---|---|---|---|---|---|
| $r_{max}$ (with $B_1$ leading) | 0.27 | 0.33 | 0.53 | 0.40 | 0.27 | 0.21 |
| lag (months) at $r_{max}$ | 2 | 5 | 28 | 27 | 36 | 39 |

## Figure Captions

Fig. 1 Negative (or reversing) feedback loop linking northern Canadian river runoff, Arctic sea-ice extent, Greenland-Iceland Sea ice extent, and salinity, convection and cyclogenesis around Iceland. This is a modified (and simplified) version of the ten-component loop originally proposed by Mysak et al. (1990) to account for interdecadal Arctic climate oscillations with periods of 15-20 years.

Fig. 2a Subregions of the Arctic Ocean and marginal seas used in the lagged cross-correlation analysis of low-pass filtered areal sea-ice extent anomalies derived from monthly sea-ice concentration (SIC) data for the period 1953-88. The dashed curve denotes the 200 m isobath.

Fig. 2b Low-pass filtered anomalies of areal sea-ice extent for subregions $B_1$, ... ,$D_1$ in the Arctic Ocean and Greenland-Iceland Sea (see Fig. 2a); note that the vertical scale in the bottom time series (for subregion $D_1$) has been compressed by a factor of five. The distances between the zero-means of adjacent pairs of time series are proportional to the corresponding distances between the centers of the adjacent subregions shown in a). The dashed lines with negative slope ($L_1$) indicate the propagation of ice anomalies from the Beaufort Sea (subregion $B_1$) through to the Greenland-Iceland Sea (subregion $D_1$). In particular, the line $L_4$ shows that the origin of the GIASA in the Greenland-Iceland Sea in the late 1980s could have been due to the large anomaly in subregions $B_1$ in the mid-1980s.

Fig. 3 a) Annual Mackenzie River runoff during 1973-89 at Arctic Red River (a city on the Mackenzie R.). (Data courtesy of R. Lawford.) b) Salinities at 1 m over the southeastern Beaufort Sea continental shelf (in subregion $B_1$) for July, August and September during 1950-87 (from Fissel and Melling 1990). c) Low-pass filtered ice anomalies in the Beaufort Sea.

Fig. 4 a) Annual mean climatology of sea-ice coverage in the Arctic Ocean and marginal seas for 1953-88 (from Mysak and Wang 1991). The centre of the black band to the east of Greenland, say, is regarded as the position of the 'ice edge' in the Greeland-Iceland Sea. b) As in a) but for 1985 (ie, average of monthly SIC data for Jan. 1985 to Dec. 1985). c) As in b) but for 1987. d) Annual mean climatology of sea-level pressure (SLP) field poleward of 45°N for 1953-87 (from Mysak and Wang 1991). Contour interval is 2 mb. e) Left, as in d) but for 1985. Right, anomaly field of the 1985 SLP shown at left expressed as departures from the climatology in d). Contour interval is 1 mb. f) As in e) but for 1987.

Fig. 5 a) As in Fig. 4b but for 1964. b) As in Fig. 4b but for 1968. c) As in Fig. 4e but for 1964. d) As in Fig. 4e but for 1968.

Fig. 6 a) Winter (Dec., Jan., Feb.) mean climatology of SLP field poleward of 45°N for 1953-88 (from Mysak and Wang 1991). Contour interval is 2 mb. b) Left, as in a) but for 1961. Right, anomaly of winter 1961 SLP field shown at left expressed as departures from the climatology in a). Contour interval is 1 mb. c) As in b), but for 1964.

Fig. 7 Best linear fit to the lag at maximum correlation (data from Table 1) versus distance from the centre of subregion $B_1$ to centre of subregion $D_3$ via the centres of subregions $B_2$, $B_3$, $B_4$, $D_1$ and $D_2$ (see Fig. 2a).

Fig. 8a Ice anomaly advection pattern derived from asymmetries about zero-lag of cross-correlation functions computed using monthly data from adjacent US Navy/NOAA Joint Ice Center standard subregions (from Chapman and Walsh 1991). Large (small) arrows connect adjacent subregions for which cross-correlations at lags+1 (month) and -1 differ by more that 0.12 (0.06). Arrows point in direction of advection implied by asymmetry.

Fig. 8b As in a) except based on cross-correlation functions using low-pass filtered data from subregions in Fig. 2a. However, in this figure a large arrow connects two subregions for which the maximum of the (asymmetric) lagged cross-correlation is significant at the 95% level. A large bar connects two subregions for which the cross-correlation function is symmetric about zero-lag, at which however, the anomalies are significantly correlated. A small

arrow connects two subregions for which the maximum of the lagged cross-correlation coefficient $r \geq 0.15$, but is not significant.

Fig. 9 Low-pass filtered and detrended SST anomalies in the latitude band 45-55°N as a function of time and latitude in the North Atlantic and Baltic Sea (from Bryan and Stouffer 1991). Solid and dotted lines next to the time axis indicate, respectively, periods of relatively large and small (or near normal) sea-ice extents in the Greenland Sea as estimated from data shown in Figs. 3, 10 and 15 in Mysak et al. (1990).

Fig. 10 The first three empirical orthogonal function (EOF) patterns of SST calculated for the period 1901-80 from the British Meteorological Office file (from Bryan and Stouffer (1991) who contoured and replotted the 10° x 10° EOF values originally computed by Folland et al. (1986a)).

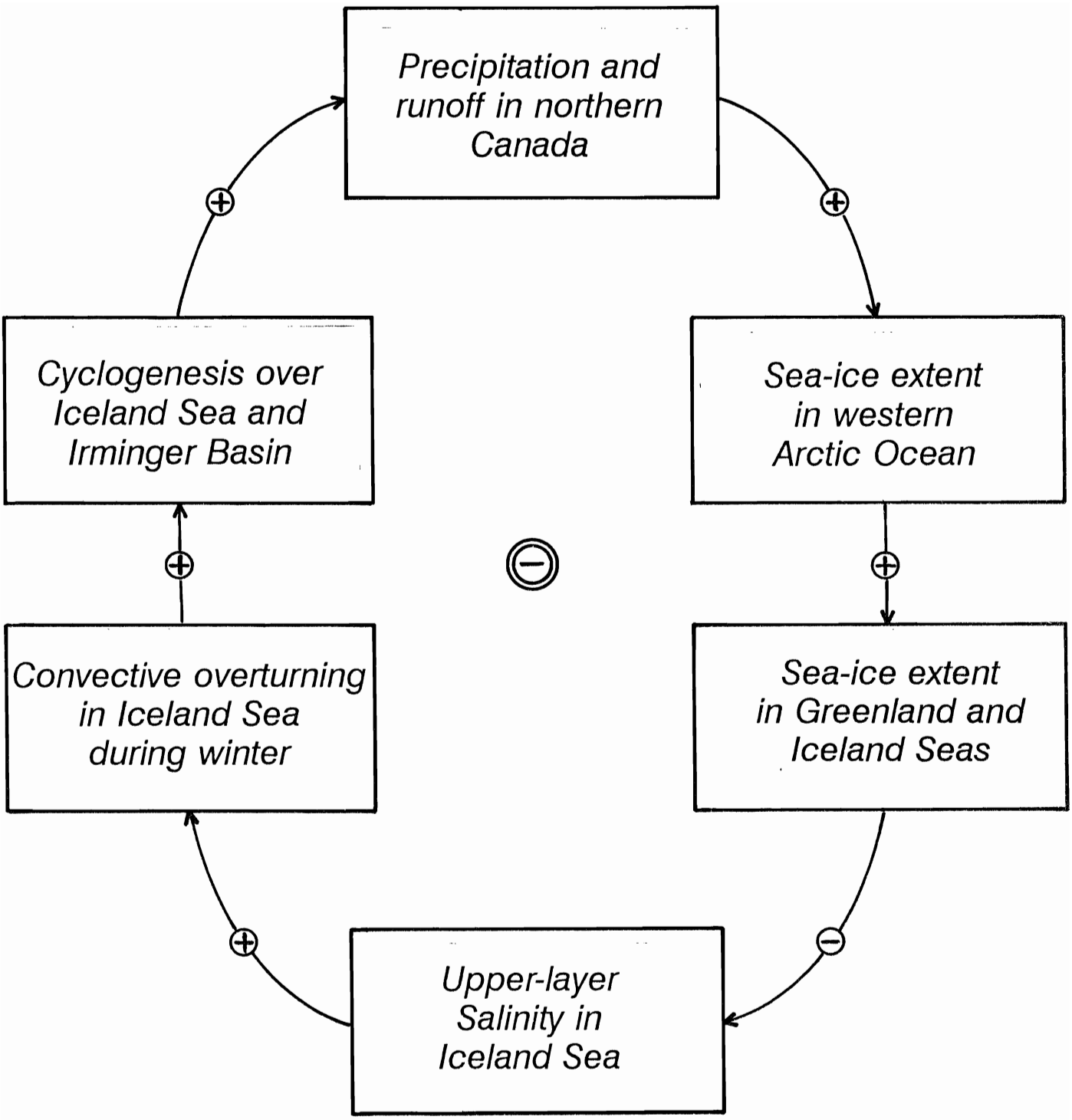
Precipitation and runoff in northern Canada
Sea-ice extent in western Arctic Ocean
Sea-ice extent in Greenland and Iceland Seas
Upper-layer Salinity in Iceland Sea
Convective overturning in Iceland Sea during winter
Cyclogenesis over Iceland Sea and Irminger Basin
⊕
⊕
⊕
⊖
⊕
⊕
⊖
⊕

# *SEA-ICE SUBREGIONS*

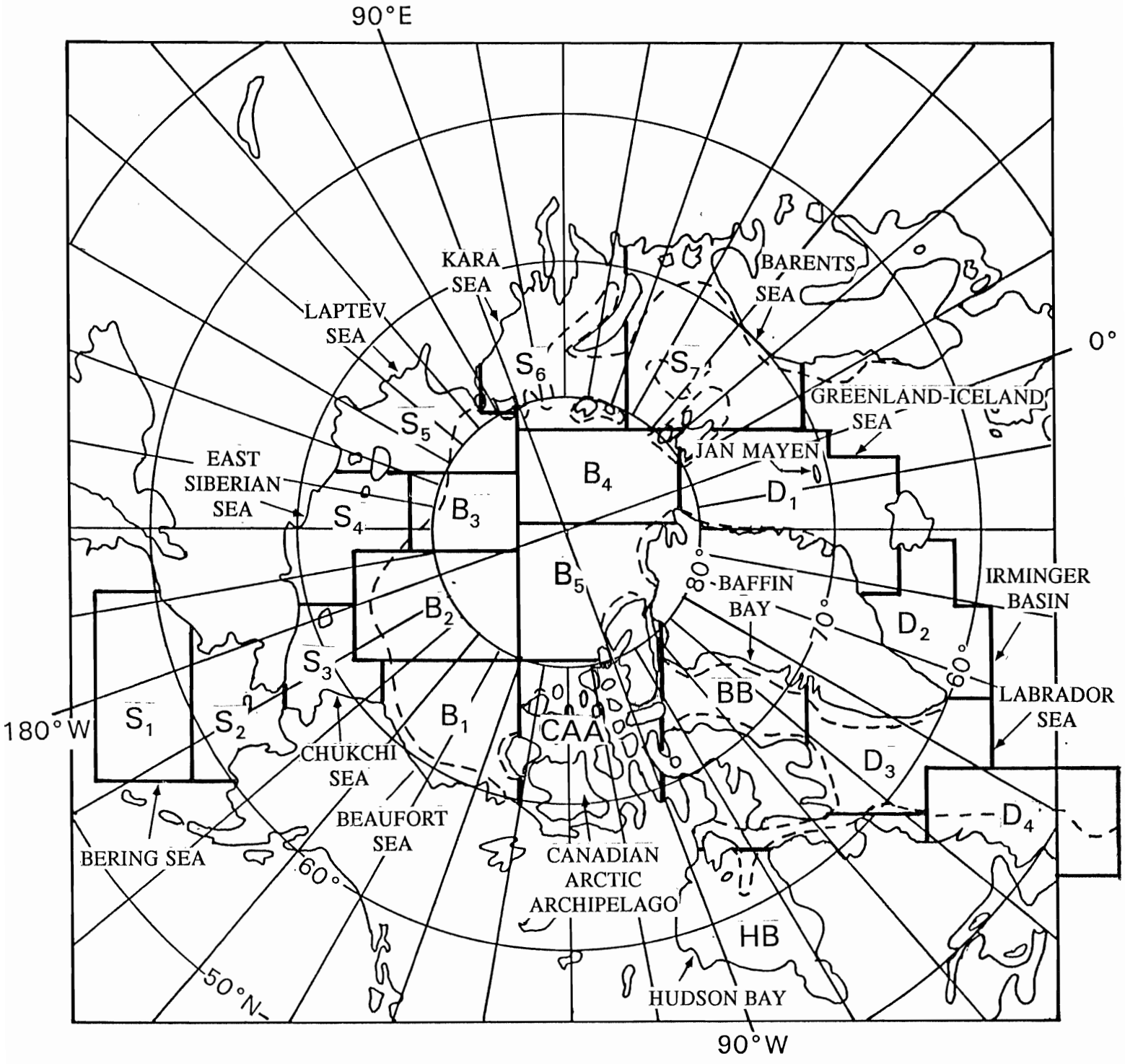

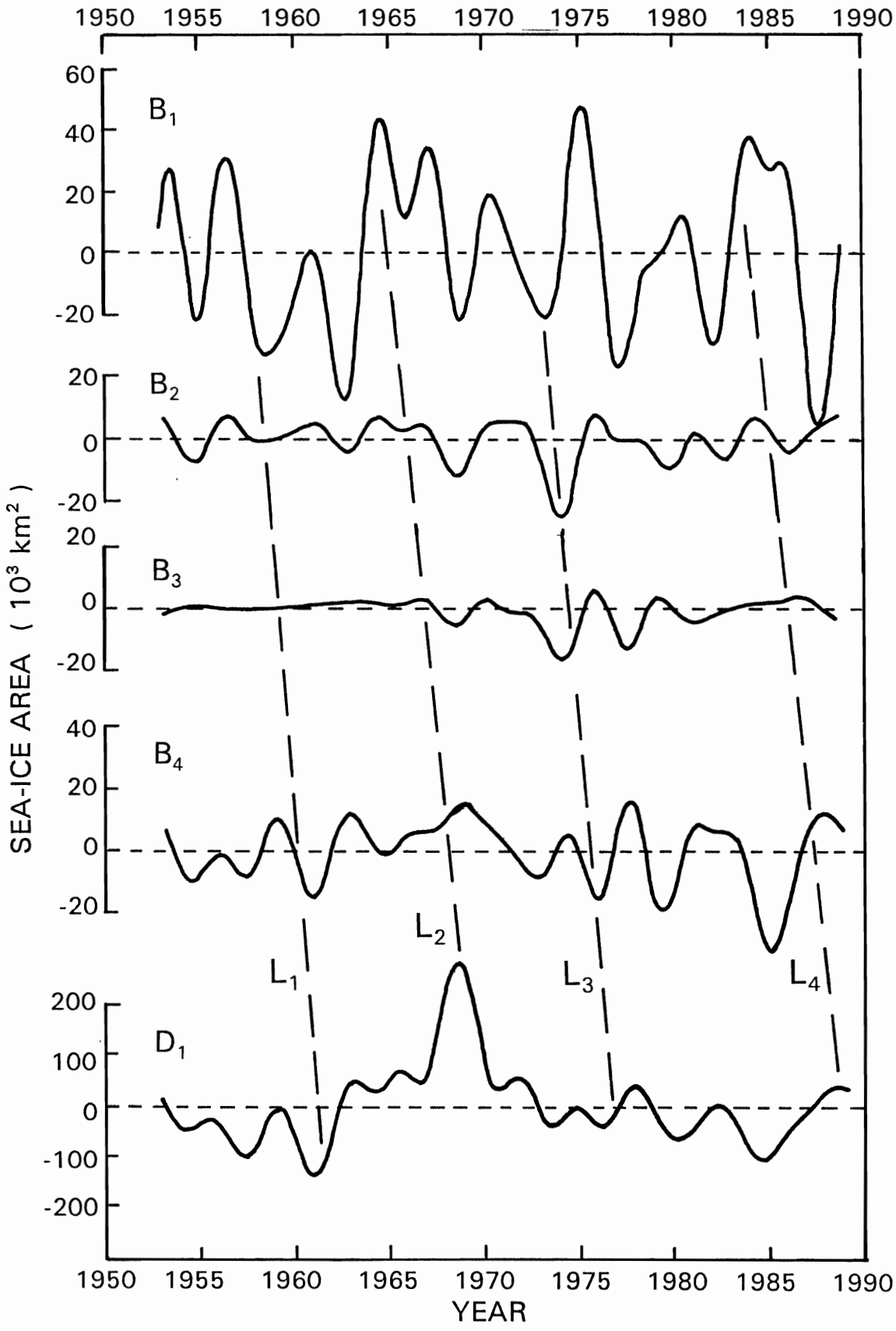
1950
1955
1960
1965
1970
1975
1980
1985
1990
B1
B2
B3
B4
D1
60
40
20
0
-20
20
0
-20
20
0
-20
40
20
0
-20
200
100
0
-100
-200
L1
L2
L3
L4
SEA-ICE AREA ( 10³ km² )
YEAR

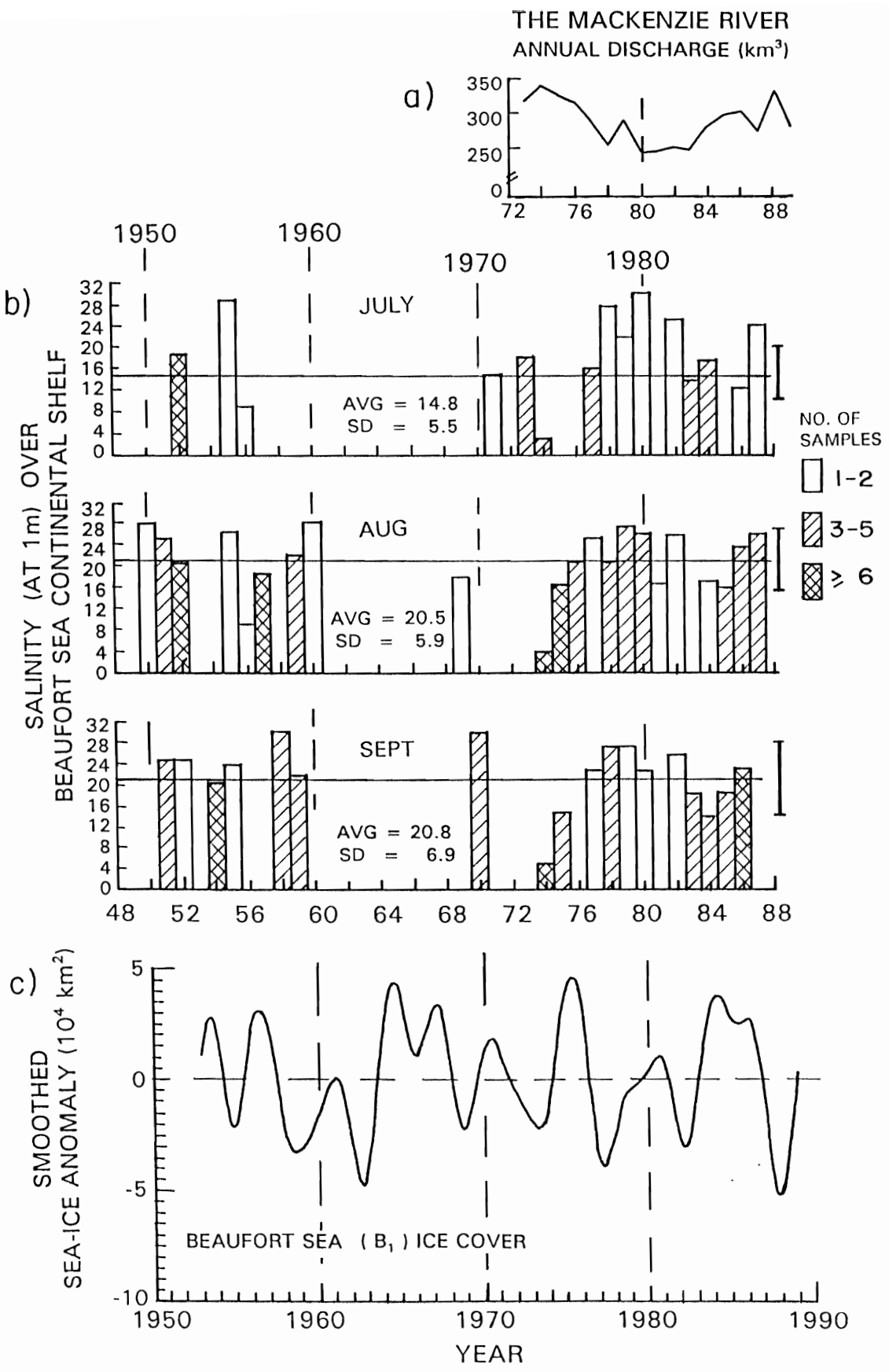
THE MACKENZIE RIVER
ANNUAL DISCHARGE (km³)
a)
350
300
250
0
72
76
80
84
88
1950
1960
1970
1980
b)
JULY
AVG = 14.8
SD = 5.5
AUG
AVG = 20.5
SD = 5.9
SEPT
AVG = 20.8
SD = 6.9
SALINITY (AT 1m) OVER
BEAUFORT SEA CONTINENTAL SHELF
NO. OF
SAMPLES
1-2
3-5
≥ 6
48
52
56
60
64
68
72
76
80
84
88
c)
SMOOTHED
SEA-ICE ANOMALY (10⁴ km²)
5
0
-5
-10
BEAUFORT SEA ( B1 ) ICE COVER
1950
1960
1970
1980
1990
YEAR

3

SEA-ICE CONCENTRATION IN TENTHS

1 —— 4-6 ▬▬ 7-9 ≡≡≡ 10 ⁝⁝⁝⁝

a)

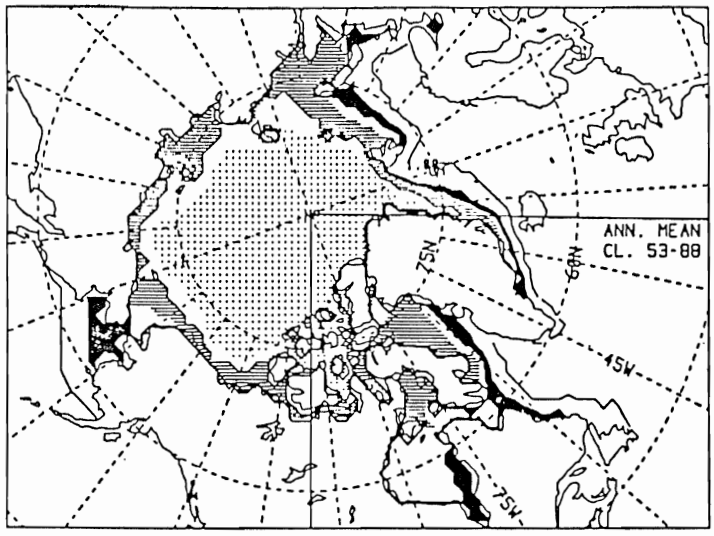


b)

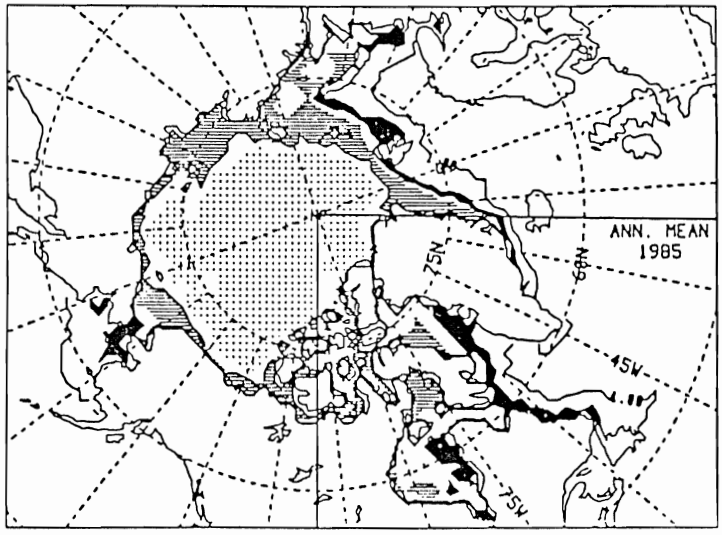


c)

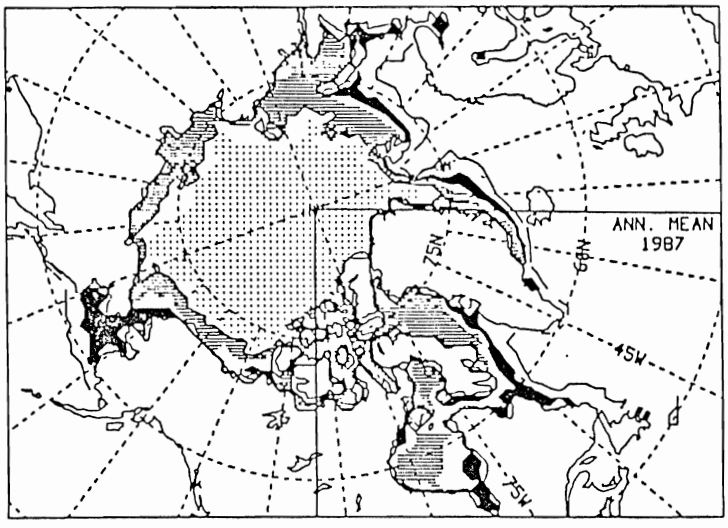


4

a, b, c

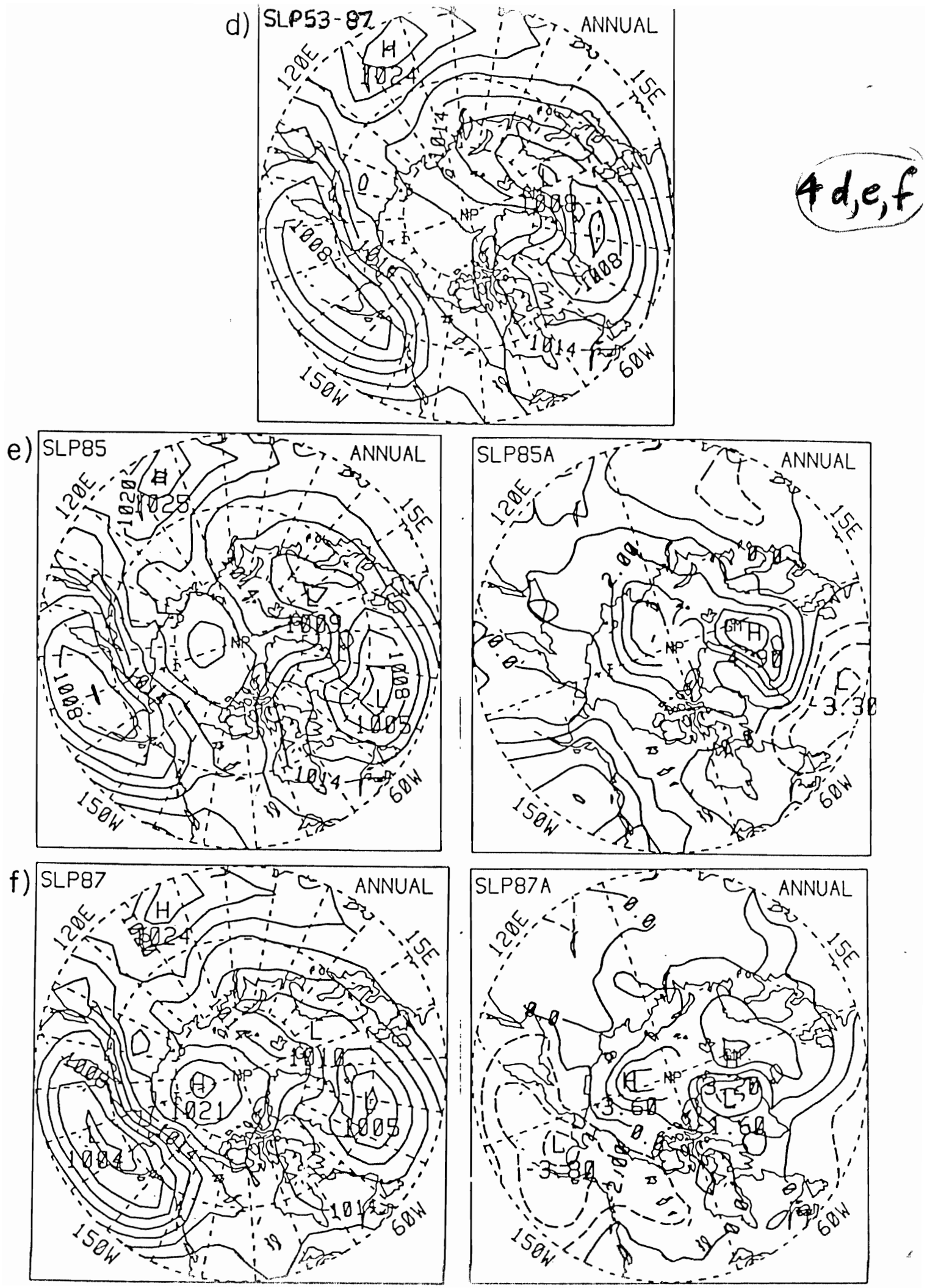
d)
SLP53-87
ANNUAL
120E
15E
H
1024
1014
1008
L
1008
1014
60W
150W
NP
e)
SLP85
ANNUAL
120E
15E
H
1020
1028
1008
1008
1009
L
1008
1005
1014
60W
150W
NP
SLP85A
ANNUAL
120E
15E
2.00
0.0
GM
H
3.30
60W
150W
NP
f)
SLP87
ANNUAL
120E
15E
H
1024
1008
L
1010
H
1021
1004
1005
1014
60W
150W
NP
SLP87A
ANNUAL
120E
15E
0.0
H
3.60
L
3.50
1.50
3.30
60W
150W
NP

4 d,e,f

SEA-ICE CONCENTRATION IN TENTHS

1 —— 4-6 ▬▬ 7-9 ≡≡≡ 10 ⁝⁝⁝⁝

a)

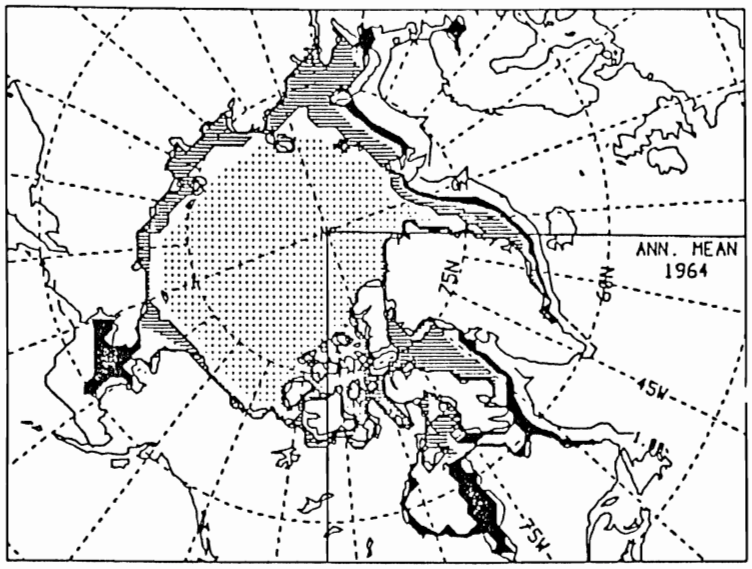


b)

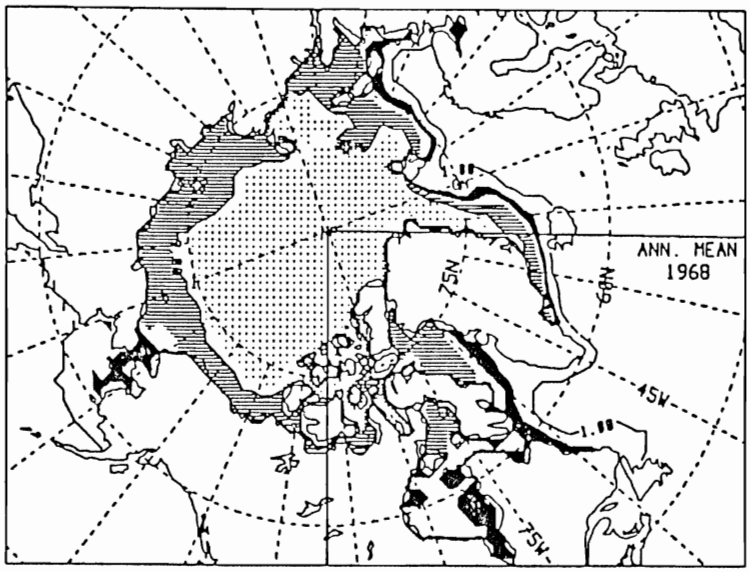


5a,b

c)

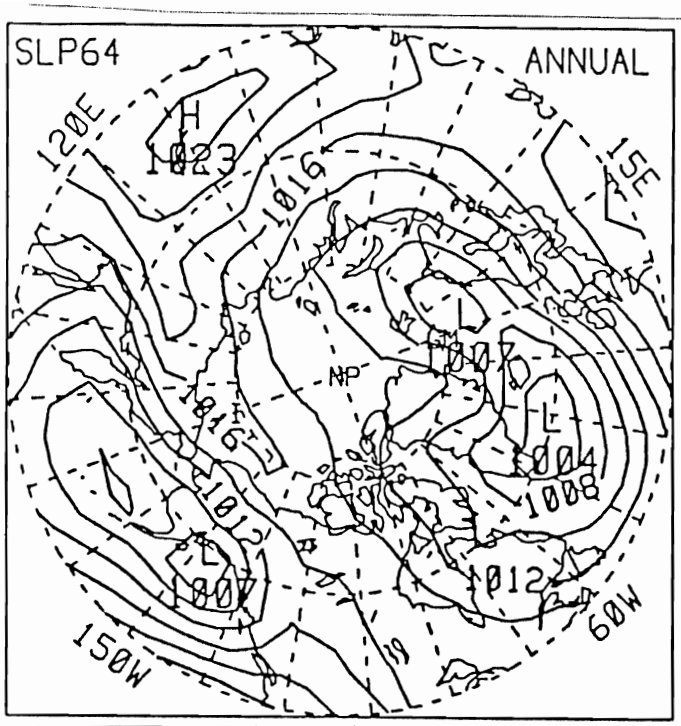
SLP64
ANNUAL
120E
15E
60W
150W
NP
H
1023
1016
1012
1008
1004
1000
L

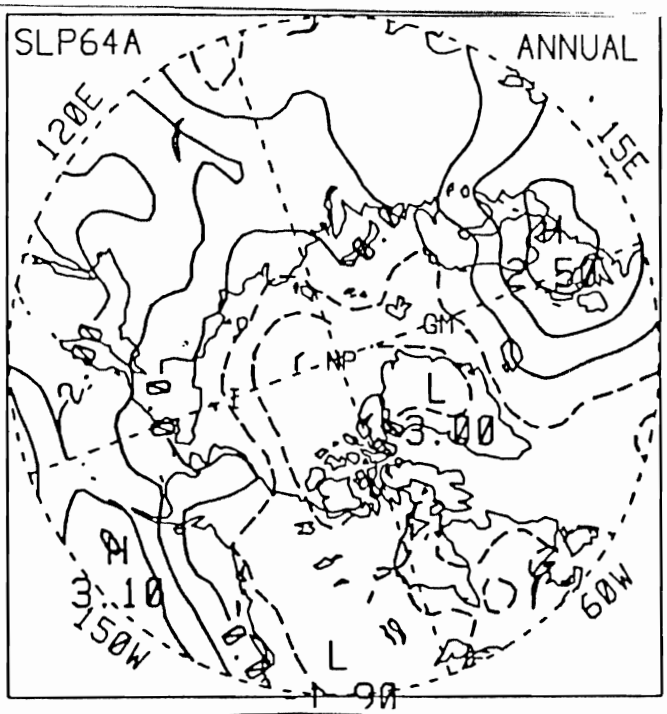
SLP64A
ANNUAL
120E
15E
60W
150W
NP
GM
L
3.00
5.0
2.0
3.10
0.0
9.0

d)

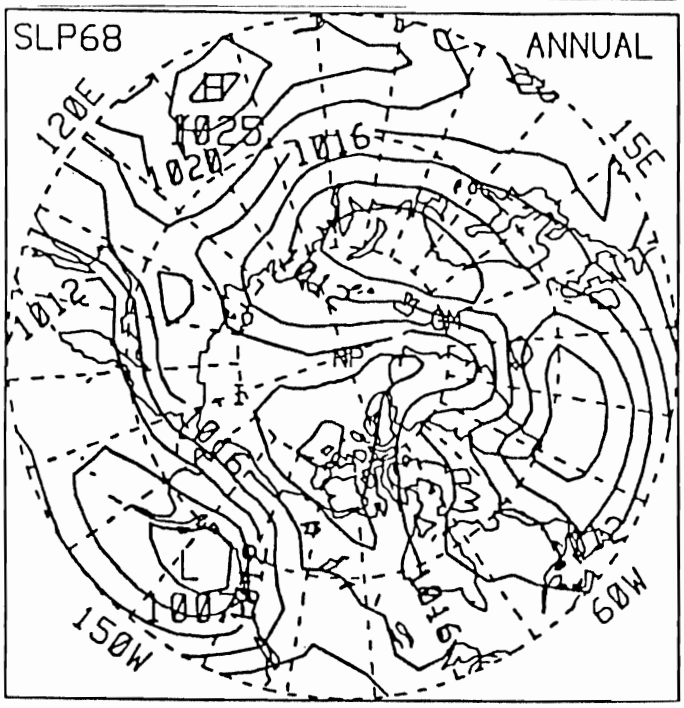
SLP68
ANNUAL
120E
15E
60W
150W
NP
1025
1020
1016
1012
1008
L

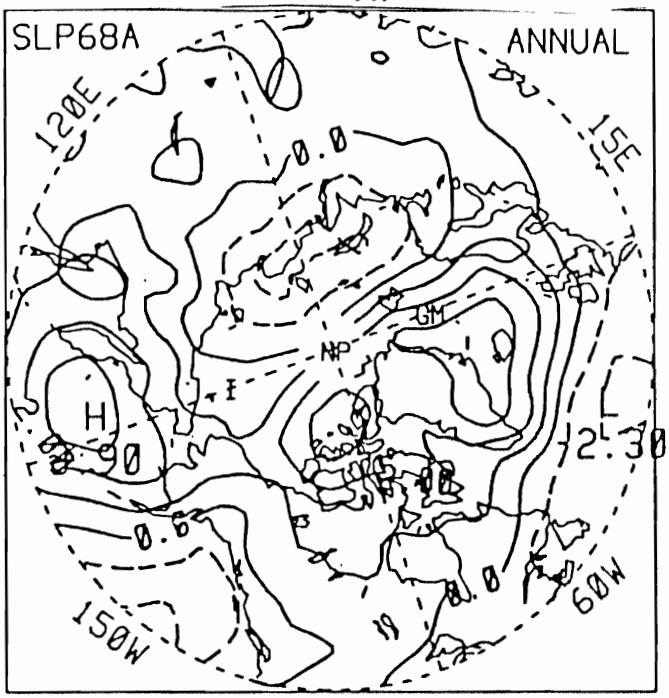
SLP68A
ANNUAL
120E
15E
60W
150W
NP
GM
0.0
H
0.90
L
2.30
0.6

5 c,d

6

a,b,c

a)

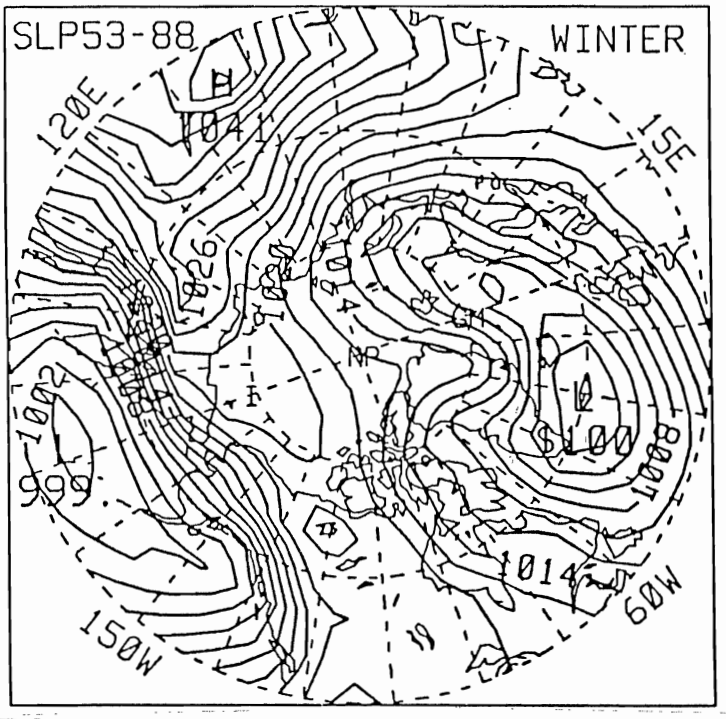
SLP53-88
WINTER
120E
15E
60W
150W
1041
1026
1014
1002
999
1008
1014

b)

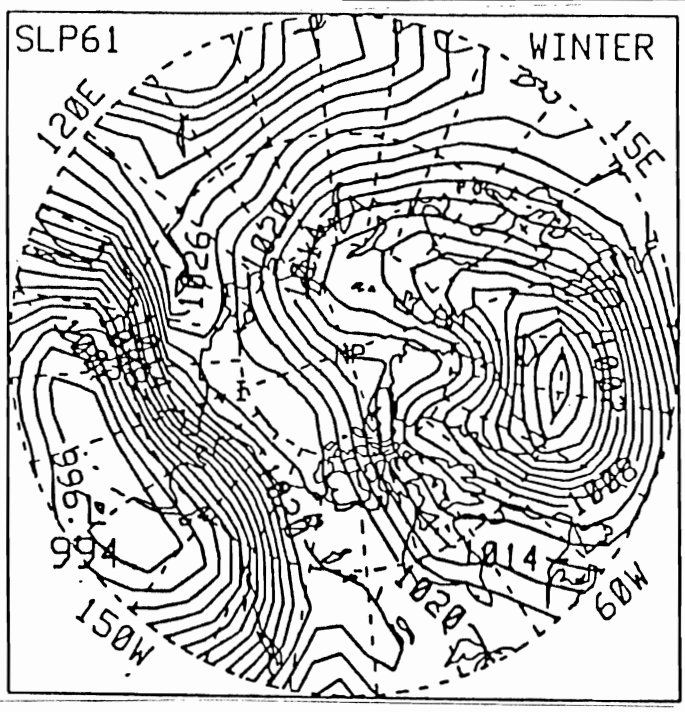
SLP61
WINTER
120E
15E
60W
150W
1026
1020
1008
1014
996
994

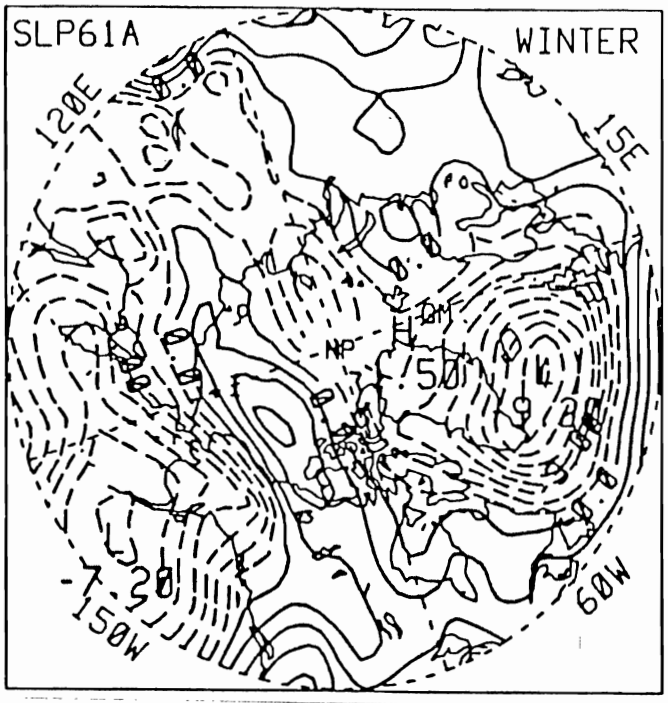
SLP61A
WINTER
120E
15E
60W
150W
-.50
-.20

c)

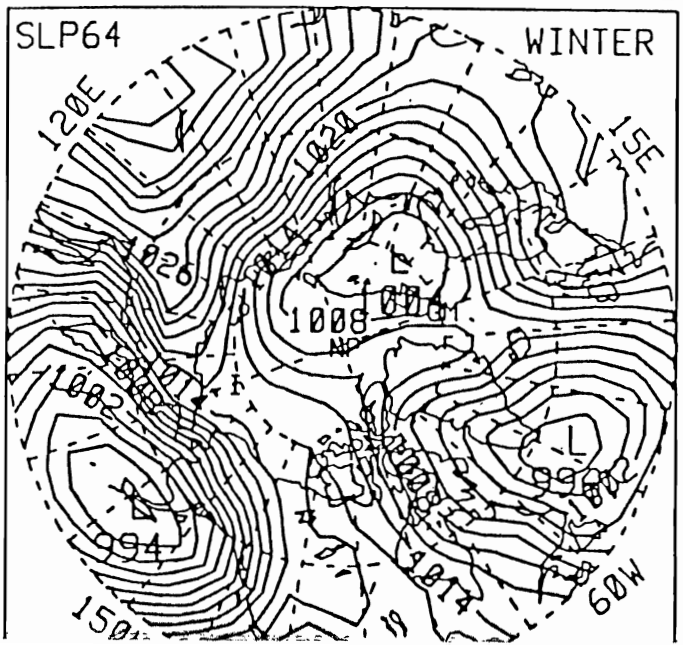
SLP64
WINTER
120E
15E
60W
1020
1026
1008
1002
994
1014

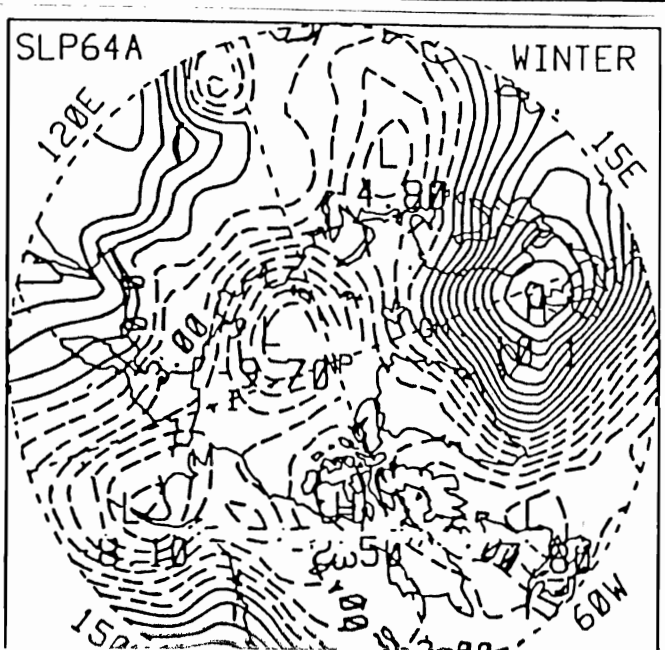
SLP64A
WINTER
120E
15E
60W
4.00
3.00
1.20
-.80

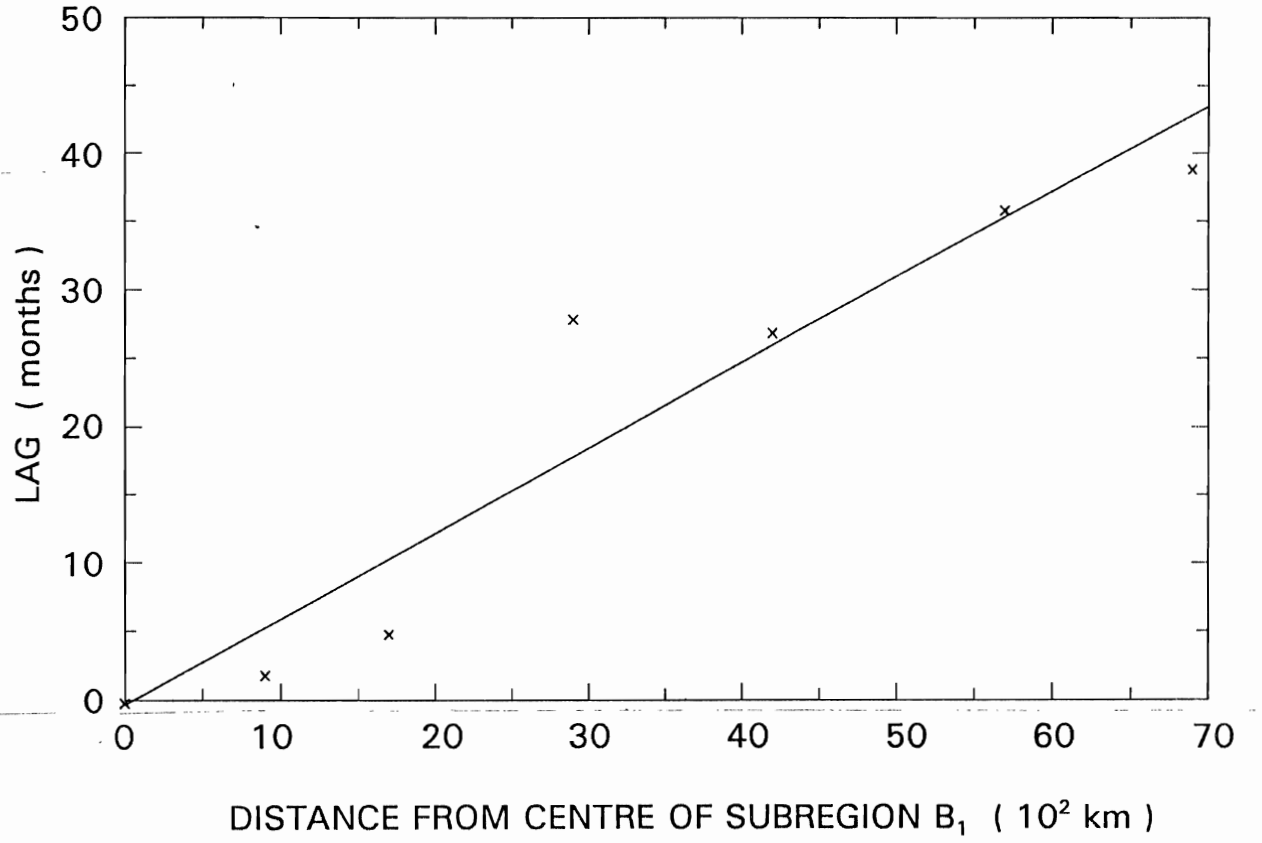
50
40
30
20
10
0
LAG ( months )
0
10
20
30
40
50
60
70
DISTANCE FROM CENTRE OF SUBREGION $B_1$ ( $10^2$ km )

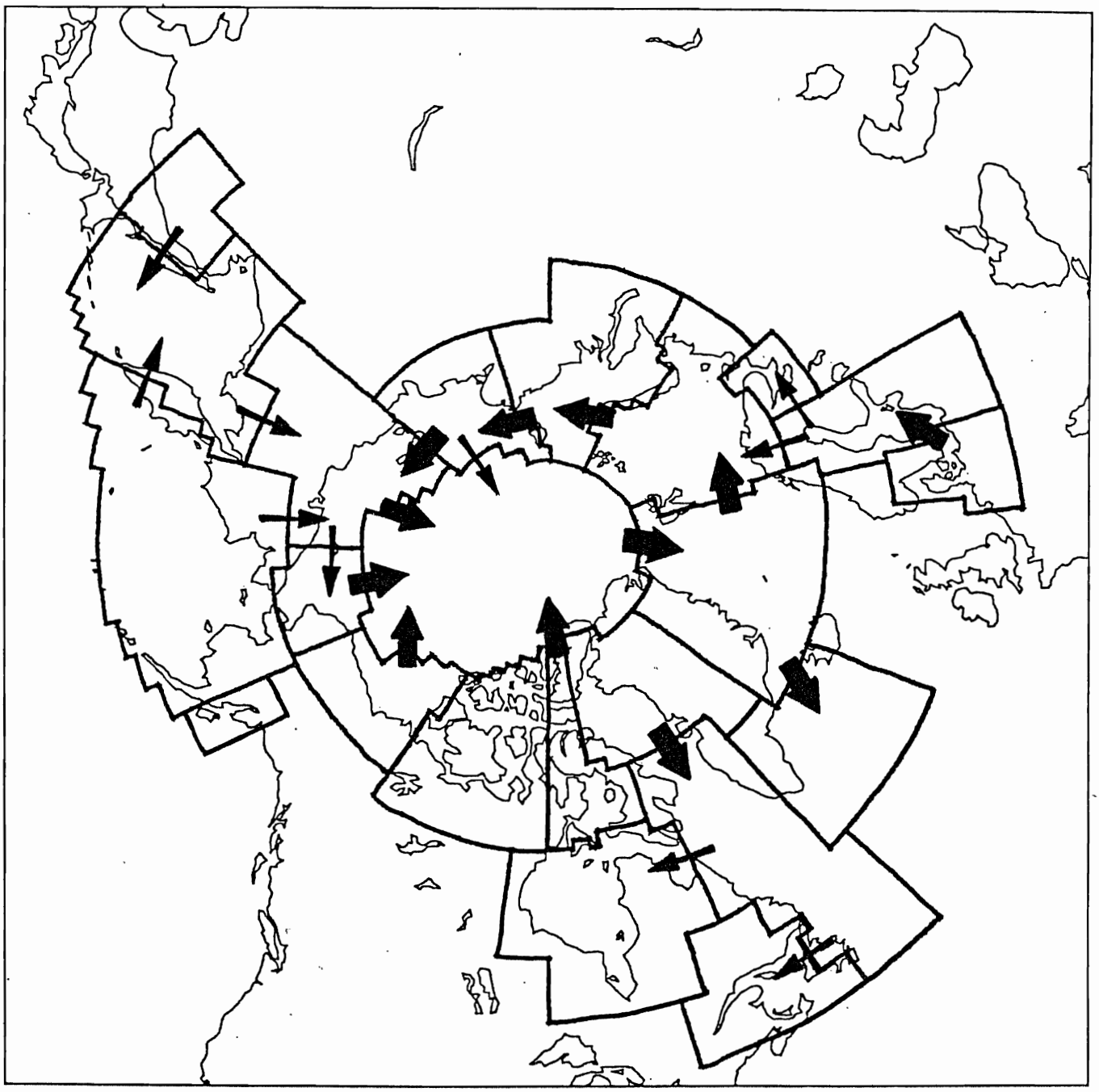

8a

# *ICE ANOMALY ADVECTION PATTERN*

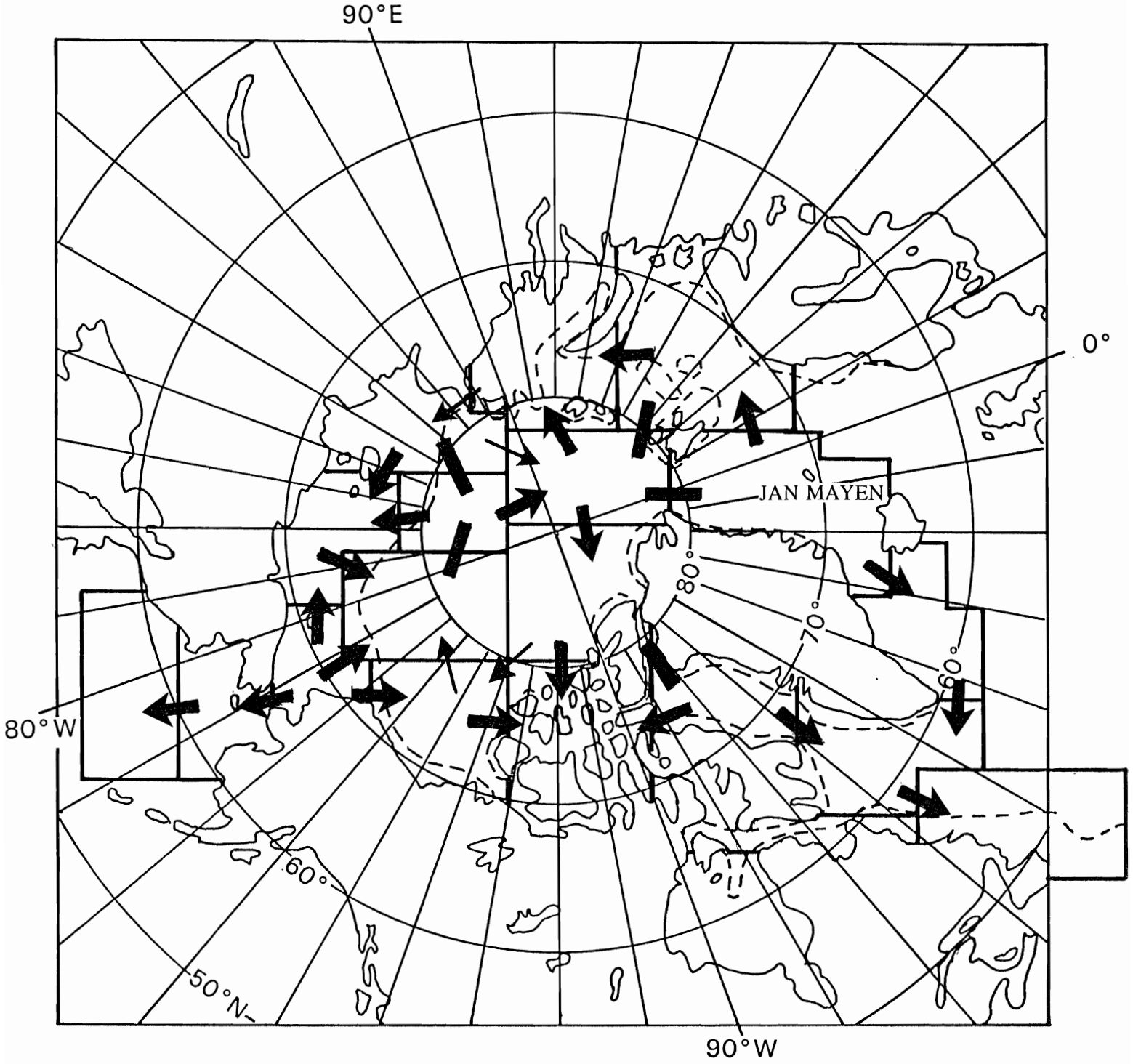


8b

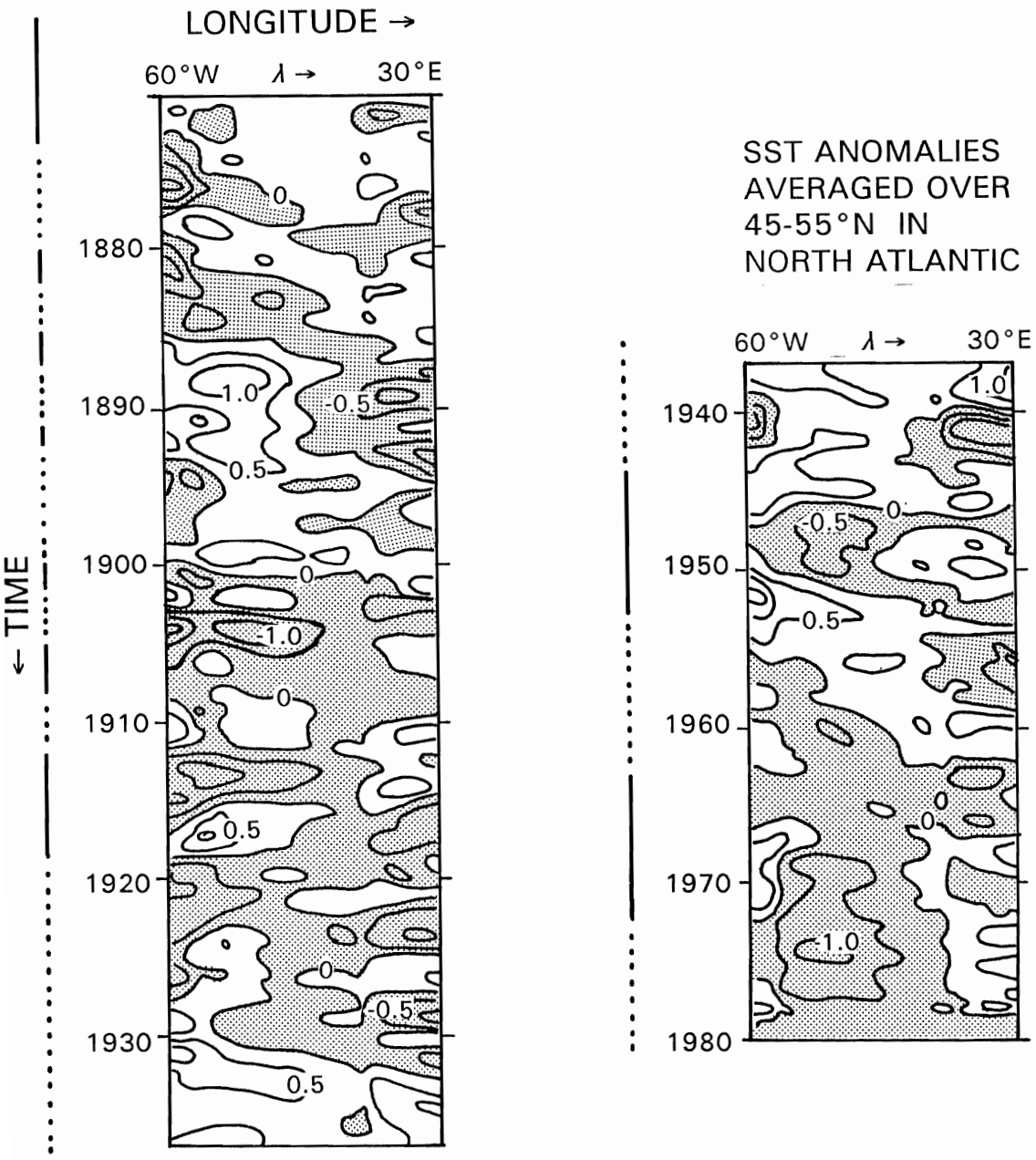


ICE CONDITIONS IN GREENLAND AND ICELAND SEAS

——— LARGE SEA-ICE EXTENT

..... SMALL OR AVERAGE SEA-ICE EXTENT

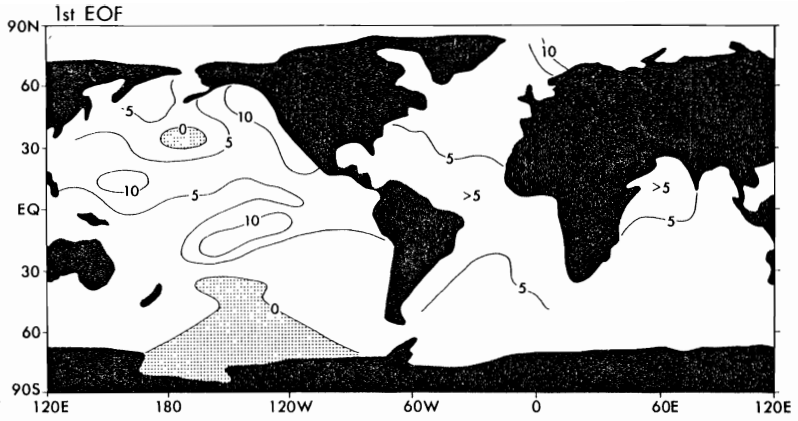
1st EOF
90N
60
30
EQ
30
60
90S
120E
180
120W
60W
0
60E
120E
10
5
0
10
5
10
5
>5
>5
5
10
5
0

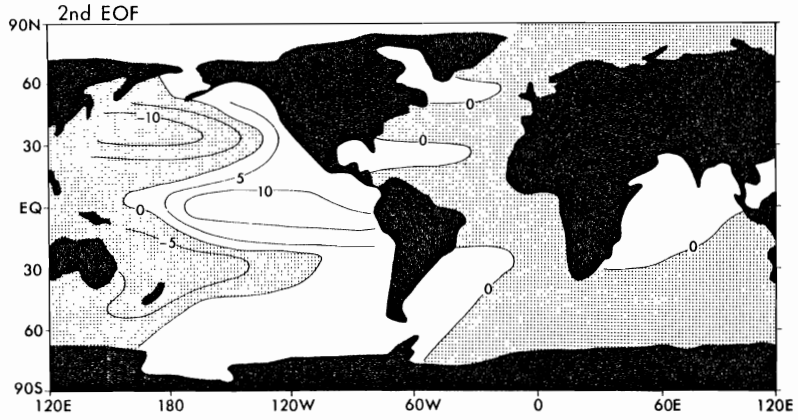
2nd EOF
90N
60
30
EQ
30
60
90S
120E
180
120W
60W
0
60E
120E
0
10
0
0
5
10
0
5
0
0

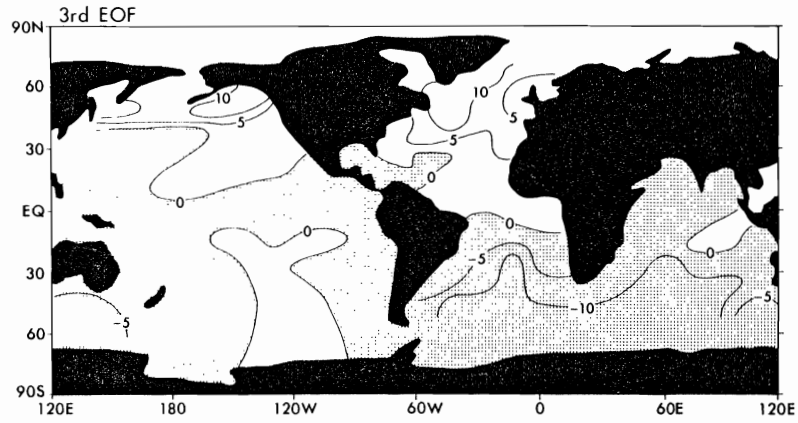
3rd EOF
90N
60
30
EQ
30
60
90S
120E
180
120W
60W
0
60E
120E
10
5
10
5
5
0
0
0
0
5
10
5
5